Dartmouth College

Dartmouth Digital Commons

Dartmouth Scholarship

Faculty Work

3-25-2011

Dynamical Critical Scaling and Effective Thermalization in Quantum Quenches: Role of the Initial State

Shusa Deng
Dartmouth College

Gerardo Ortiz
University of Indiana

Lorenza Viola
Dartmouth College

Follow this and additional works at: https://digitalcommons.dartmouth.edu/facoa

Part of the Quantum Physics Commons

Dynamical critical scaling and effective thermalization in quantum quenches: Role of the initial state

Shusa Deng,[1] Gerardo Ortiz,[2] and Lorenza Viola[1]

[1]*Department of Physics and Astronomy, Dartmouth College, Hanover, New Hampshire 03755, USA*
[2]*Department of Physics, University of Indiana, Bloomington, Indiana 47405, USA*

We explore the robustness of universal dynamical scaling behavior in a quantum system near criticality with respect to initialization in a large class of states with finite energy. By focusing on a homogeneous XY quantum spin chain in a transverse field, we characterize the nonequilibrium response under adiabatic and sudden quench processes originating from a pure as well as a mixed excited initial state, and involving either a regular quantum critical or a multicritical point. We find that the critical exponents of the ground-state quantum phase transition can be encoded in the dynamical scaling exponents despite the finite energy of the initial state. In particular, we identify conditions on the initial distribution of quasiparticle excitation that ensure that Kibble-Zurek scaling persists. The emergence of effective thermal equilibrium behavior following a sudden quench toward criticality is also investigated, with focus on the long-time expectation value of the quasiparticle number operator. Despite the integrability of the XY model, this observable is found to behave thermally in quenches to a regular quantum critical point, provided that the system is initially prepared at sufficiently high temperature. However, a similar thermalization behavior fails to occur in quenches toward a multicritical point. We argue that the observed lack of thermalization originates in this case in the asymmetry of the impulse region that is also responsible for anomalous multicritical dynamical scaling.

I. INTRODUCTION

Characterizing the nonequilibrium dynamics of quantum many-body systems is of central significance to both condensed-matter physics and quantum statistical mechanics. A quantitative understanding of nonequilibrium quantum phase transitions (QPTs) is, in particular, a fundamental prerequisite for uncovering and controlling quantum phases of matter,[1,2] as well as for assessing the complexity of quantum annealing or adiabatic algorithms.[3,4] Unlike standard phase transitions, which are driven by a change in temperature, QPTs are driven entirely by quantum fluctuations at zero temperature. They nevertheless share with their classical counterpart the generic feature of universality: In equilibrium, the critical properties of a system sufficiently close to a quantum critical point (QCP) depend only on a few relevant characteristics such as its symmetry and dimensionality, thus defining the universality class to which the corresponding (continuous) QPT belongs. The universality class is distinguished by a small set of critical exponents, for instance, ν and z, describing the power-law divergence of the characteristic length scale and the vanishing of the characteristic energy scale, respectively.[1] In a nonequilibrium scenario, the system can be driven across a QCP *dynamically*, that is, through an explicit time dependence of one or more control parameters in the underlying many-body Hamiltonian. This naturally prompts a number of questions: To what extent can universal quantum scaling laws persist out of equilibrium and be solely specified in terms of the equilibrium phase diagram? Conversely, how does quantum criticality influence the ability of a system to relax back to equilibrium?

Historically, the first theoretical studies in these directions date back to the pioneering work by Barouch and co-workers[5–7] which led, in particular, to the discovery of "nonergodic" behavior in the zero-temperature long-time magnetization of a driven XY spin chain.[6] In recent years, the demand for quantitatively addressing the above broad questions has heightened under the impetus of experimental advances in manipulating ultracold atomic gases, which are enabling the unitary dynamics of many-body quantum systems to be explored with an unprecedented level of coherent control and isolation from the environment.[8,9] As a result, nonequilibrium quantum critical physics is being actively investigated both from theoretical and experimental standpoints.

In this framework, an important step forward is provided by the prediction of universal behavior in *adiabatic* dynamics near a QCP based on the *Kibble-Zurek scaling* (KZS) argument[10] (see also Ref. 11 for related independent work and Ref. 12 for a recent review). Originally introduced in the context of classical (finite-temperature) phase transitions in cosmology,[13] the KZ argument rests on the basic intuition that, irrespective of how slowly a system is driven across a continuous phase transition, adiabaticity is necessarily lost in the thermodynamic limit due to the vanishing energy gap at the critical point. Qualitatively, this determines typical time and length scales, $\hat{t}$ and $\hat{\xi}$, respectively, which characterize the adiabatic-to-diabatic crossover and, since "order" cannot be established on distances larger than $\hat{\xi}$, results in the formation of a domain structure and the generation of a *finite* density of "topological defects" in the system. Quantitatively, let the time dependence in the quantum-mechanical Hamiltonian $H(t)$ be introduced through a control parameter $\lambda(t)$, with $\lambda_c \equiv \lambda(t_c)$ corresponding to the crossing of an isolated QCP at time t_c, which can be taken to be $t_c \equiv 0$ without loss of generality. If the system is initially ($t = t_0$) in the ground state, its ability to adiabatically adjust to $H(t)$ is determined by the condition that the typical time scale $\tau(t) \equiv |(\lambda(t) - \lambda_c)/\dot{\lambda}(t)|$ associated with the applied control be sufficiently long relative to the slowest response time $\tau_r \sim \Delta^{-1}$, which is set by the smallest energy gap Δ. Since, as the QCP is approached, the latter vanishes as $\Delta \sim |\lambda(t) - \lambda_c|^{\nu z}$, adiabaticity is broken throughout an
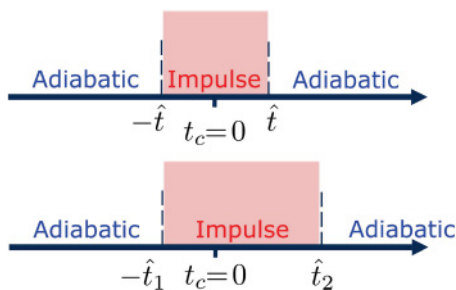
FIG. 1. (Color online) Qualitative sketch of the adiabatic-impulse-adiabatic sequence of regimes relevant to dynamical scaling arguments. Top: Symmetric impulse region, as assumed by the standard KZS scenario. Bottom: Asymmetric impulse region, as resulting from the existence of quasicritical path-dependent energy states; see Ref. 23.

"impulse region" $[t_c - \hat{t}, t_c + \hat{t}]$ symmetrically located around the QCP, where the "freeze-out" time $\hat{t}$ is determined by the condition $\tau(\hat{t}) = \tau_r(\hat{t})$. In the simplest case of a linear sweep across the QCP (Fig. 1, top), $\lambda(t) - \lambda_c \equiv t/\tau$ for a fixed rate $\tau^{-1} > 0$, this yields $\hat{t} \sim \tau^{\nu z/(\nu z+1)}$ and a typical gap $\hat{\Delta} \sim \hat{t}^{-1}$. Correspondingly, the typical correlation length $\hat{\xi} \sim \xi(\hat{t}) \sim \hat{\Delta}^{-z}$ also scales with the quench time τ. Since $\hat{\xi}$ is the universal length scale near criticality, it determines the scaling of the final ($t = t_f$) density of defects and, more generally, the *total* density of excitations, $n_{\text{ex}}(t_f)$, created in the system. If d denotes the spatial dimension, the KZS result then follows:

$$n_{\text{ex}}(t_f) \sim \tau^{-d\nu/(\nu z+1)}. \qquad (1)$$

The validity as well as the limitations of the above KZS have been carefully scrutinized in a number of settings. By now, the original KZS has been confirmed for a variety of models involving a regular isolated QCP,[14–18] and extensions have been introduced for more general adiabatic dynamics, including repeated,[19] nonlinear,[20] and optimal[21] quench processes. In parallel, departures from the KZS predictions have emerged for more complex adiabatic scenarios, involving, for instance, quenches across either an isolated multicritical point (MCP),[20,22–25] or nonisolated QCPs (that is, critical regions),[26–29] as well as QPTs in infinitely coordinated,[30] disordered,[31] and/or spatially inhomogeneous systems.[12,32] A main message that has emerged from the above studies is that, unlike in the standard KZS of Eq. (1) where the nonequilibrium critical exponent is completely specified in terms of static exponents, additional details about the time-dependent excitation may play an essential role in general. As a result, genuinely nonstatic, *path-dependent exponents* may be required for dynamical scaling predictions. This feature is vividly exemplified, for instance, in multicritical quantum quenches, whereby the asymmetry of the KZ impulse region relative to the static QCP (Fig. 1, bottom) causes a path-dependent minimum gap other than the critical gap to be relevant and an effective dynamical exponent $z_2 \neq z$ to emerge.[23]

In addition to characterizing the response to an adiabatic probe, the opposite limit of a *sudden* change of the tuning parameter $\lambda(t)$ near a QCP has also attracted a growing attention recently, in connection with the study of both dynamical quantum-critical properties,[33–35] as well as thermalization dynamics in closed quantum systems and its

interplay with quantum integrability.[36–43] In particular, for sudden quenches with a sufficiently *small amplitude*, the existence of universal scaling behavior has been established for various physical observables and qualitatively related to the above KZ argument:[35,44] by associating to a quench with amplitude $\delta\lambda$ the characteristic length scale $\xi \sim |\delta\lambda|^{-\nu}$, and by interpreting ξ as the correlation length in the final state, one immediately infers that $n_{\text{ex}}(t_f) \sim \xi^{-d} \sim |\delta\lambda|^{d\nu}$.

With a few exceptions where quenches at finite temperature and the associated thermal corrections have also been examined,[35,36,44,45] the large majority of the existing investigations have focused on quench dynamics originating from the ground state of the initial Hamiltonian $H(t_0)$. Our goal in this work is to present a dedicated analysis of *finite-energy quantum quenches*, with a twofold motivation in mind. Conceptually, elucidating to what extent and how universal scaling properties may depend upon the details of the system's initialization is needed to gain a more complete picture of nonequilibrium quantum-critical physics. While one might, for instance, naively expect that a sizable overlap with the initial ground state would be essential in determining the applicability of ground-state scaling results, a main highlight of our analysis is that the support of the initial state on those excitations relevant to the path-dependent excitation process is key in a dynamical scenario, in a sense to be made precise later. Furthermore, from a practical standpoint, perfect initialization of a many-body Hamiltonian in its exact ground state is both non-deterministic polynomial (NP)-hard in general[46,47] and experimentally unfeasible due to limited control. In this sense, our investigation both extends previous studies on finite-temperature signatures of static QPTs,[48] and may be directly relevant to experiments using ultracold atoms[8] as well as nuclear magnetic resonance (NMR) quantum simulators.[49,50]

While our analysis focuses on the simplest yet paradigmatic case of an exactly solvable XY quantum spin chain (Sec. II), we address nonequilibrium dynamics originating from a large class of (bulk) initial states for a variety of different quench schemes involving either a regular QCP or a MCP. Both pure and mixed initial states carrying finite excitation energy above the ground state are examined, under the main assumption that, subsequent to initialization, the system can be treated as (nearly) isolated, hence evolving under a time-dependent Hamiltonian. In particular, dynamical scaling in adiabatic and sudden quenches starting from an *excited energy eigenstate* are analyzed in Secs. III A and III B, respectively, with emphasis on making contact with previously introduced adiabatic renormalization approaches[15,28] and on clarifying formal connections between scaling behavior in sudden and adiabatic dynamics. The case of a *generic excited pure state* prepared by a sudden parameter quench is also considered in Sec. III C, and criteria are identified for KZS to be obeyed. Section IV is devoted to quench dynamics resulting from an *initial thermal mixture*, with the main goals of characterizing the robustness of dynamical scaling behavior in realistic finite-temperature conditions, and of further exploring the conditions leading to effective thermalization of certain physical observables following a sudden quench toward criticality. In the process, we continue and extend the analysis undertaken in Deng *et al.*[23] by presenting finite-temperature generalizations of the scaling predictions obtained for adiabatic (both linear

and nonlinear) *multicritical quantum quenches*, as well as evidence of how the peculiar nature of a MCP may also result in *anomalous thermalization behavior*. Section V concludes with a discussion of the main findings and their implications, along with further open problems.

II. MODEL HAMILTONIAN

A. Energy spectrum and equilibrium phase diagram

We consider the homogeneous one-dimensional spin-1/2 XY model described by the Hamiltonian

$$H = -\sum_{j=1}^{N}\left(\frac{1+\gamma}{2}\sigma_x^j\sigma_x^{j+1} + \frac{1-\gamma}{2}\sigma_y^j\sigma_y^{j+1} - h\sigma_z^j\right), \quad (2)$$

where periodic boundary conditions are assumed, that is, $\sigma_\alpha^j \equiv \sigma_\alpha^{j+N}$, and N is taken to be even. Here, $\gamma, h \in [-\infty, \infty]$, parametrize the degree of anisotropy in the XY plane, and the uniform magnetic-field strength, respectively, in suitable units. The diagonalization of Hamiltonian (2) is well known,[5,6,51,52] and we only recall the basic steps here. Upon introducing canonical fermionic operators $\{c_j, c_j^\dagger\}$ via the Jordan-Wigner mapping $c_j^\dagger \equiv \prod_{\ell=1}^{j}(-\sigma_z^\ell)\sigma_+^j$, H rewrites as a quadratic form

$$H = -\sum_{j=1}^{N-1}(c_j^\dagger c_{j+1} + \gamma c_j^\dagger c_{j+1}^\dagger + \text{H.c.}) + 2h\sum_{j=1}^{N}c_j^\dagger c_j$$
$$- hN + \mathcal{P}(c_N^\dagger c_1 + \gamma c_N^\dagger c_1^\dagger + \text{H.c.}), \quad (3)$$

where the last term originates from the spin periodic boundary conditions and the parity operator $\mathcal{P} \equiv \prod_{j=1}^{N}(-\sigma_z^j) = e^{i\pi\sum_{j=1}^{N}c_j^\dagger c_j} = +1(-1)$ depending on whether the eigenvalue of the total fermionic number operator is even (odd), respectively. Physically, $\mathcal{P}$ corresponds to a global $\mathbb{Z}_2$ symmetry, which, for finite N, allows the even and odd subspaces to be exactly decoupled, $H \equiv H^{(+)} + H^{(-)}$, and the diagonalization to be carried out separately in each sector.

In finite systems, the ground state as well as excited energy eigenstates with an even number of fermions belong to the $\mathcal{P} = +1$ sector. By using a Fourier transformation to momentum space, $c_k^\dagger = \frac{1}{\sqrt{N}}\sum_{j=1}^{N}e^{-ikj}c_j^\dagger$, followed by a Bogoliubov rotation to fermionic quasiparticles $\{\gamma_k, \gamma_k^\dagger\}$, with $\gamma_k = u_k c_k - i v_k c_{-k}^\dagger$, $u_k = u_{-k}$, $v_k = -v_{-k}$, and $u_k^2 + v_k^2 = 1$, the Hamiltonian in Eq. (3) rewrites as a sum of noninteracting terms:

$$H^{(+)} \equiv \sum_{k\in K_+} H_k = \sum_{k\in K_+}\epsilon_k(h,\gamma)(\gamma_k^\dagger\gamma_k + \gamma_{-k}^\dagger\gamma_{-k} - 1). \quad (4)$$

Here, the set $K \equiv K_+ + K_-$ of allowed momentum modes is determined by the antiperiodic boundary conditions on the fermions in the even sector, $c_{j+N} \equiv -c_j$, which yields $K_\pm = \{\pm\frac{\pi}{N}, \pm\frac{3\pi}{N}, \ldots, \pm(\pi - \frac{\pi}{N})\}$, and

$$\epsilon_k(h,\gamma) = 2\sqrt{(h-\cos k)^2 + \gamma^2\sin k^2} \quad (5)$$

is the quasiparticle energy of mode k. For each k, let $\mathcal{H}_k \equiv \text{span}\{|0_k\rangle, |1_k\rangle\}$, where $\{|0_k\rangle, |1_k\rangle = \gamma_k^\dagger|0_k\rangle\}$ are orthonormal states corresponding, respectively, to zero and one Bogoliubov quasiparticle with momentum k, that is, $\langle 0_k|\gamma_k^\dagger\gamma_k|0_k\rangle = 0$,

$\langle 1_k|\gamma_k^\dagger\gamma_k|1_k\rangle = 1$, and similarly for $-k$. Thus the four eigenstates of H_k provide a basis for $\mathcal{H}_k \otimes \mathcal{H}_{-k}$,

$$\mathcal{B}_k = \{|0_k, 0_{-k}\rangle, |1_k, 1_{-k}\rangle, |0_k, 1_{-k}\rangle, |1_k, 0_{-k}\rangle\}$$
$$\equiv \mathcal{B}_k^{(+)} \oplus \mathcal{B}_k^{(-)}, \quad (6)$$

where the corresponding eigenenergies are given by $-\epsilon_k, \epsilon_k$, 0, 0, and a further separation into an even (odd) sector for each k is possible due to the fact that $[\mathcal{P}_k, H_k] = 0$, with $\mathcal{P}_k \equiv e^{i\pi(\gamma_k^\dagger\gamma_k + \gamma_{-k}^\dagger\gamma_{-k})} = e^{i\pi(c_k^\dagger c_k + c_{-k}^\dagger c_{-k})}$.

The ground state of $H^{(+)}$ corresponds to the BCS state with no Bogoliubov quasiparticles,

$$|\Psi_0^{(+)}\rangle = \bigotimes_{k\in K_+}|0_k 0_{-k}\rangle = \bigotimes_{k\in K_+}(u_k + iv_k c_k^\dagger c_{-k}^\dagger)|\text{vac}\rangle,$$

where $|\text{vac}\rangle$ is the fermionic vacuum. Many-body excited states in the even sector can be obtained by applying pairs of Bogoliubov quasiparticle operators to $|\Psi_0^{(+)}\rangle$. In particular, excited eigenstates with support only on the even sector $\mathcal{B}_k^{(+)}$ for each mode are obtained by exciting only pairs of quasiparticles with opposite momentum and have the form

$$|\Psi_E^{(+)}\rangle = \left(\bigotimes_{k\in K_+^e}|1_k 1_{-k}\rangle\right)\left(\bigotimes_{k\in K_+ - K_+^e}|0_k 0_{-k}\rangle\right), \quad (7)$$

where K_+^e labels the subset of excited modes.

For finite N, the ground state and excited energy eigenstates with an odd number of fermions belong to the sector $\mathcal{P} = -1$, which implies periodic boundary conditions on the fermions, $c_{j+N} \equiv c_j$, and a different set $\bar{K}$ of allowed momentum modes, $\bar{K} \equiv \bar{K}_+ + \bar{K}_- + \{0, -\pi\}$, where $\bar{K}_\pm = \{\pm\frac{2\pi}{N}, \pm\frac{4\pi}{N}, \ldots, \pm(\pi - \frac{2\pi}{N})\}$. Since one may show that $\epsilon_{k=0} = h - 2$ and $\epsilon_{k=-\pi} = h + 2$, occupying mode 0 has always lower energy than occupying mode $-\pi$, thus the ground state of $H^{(-)}$ is now

$$|\Psi_0^{(-)}\rangle = |1_0 0_{-\pi}\rangle\bigotimes_{k\in\bar{K}_+}|0_k 0_{-k}\rangle,$$

and excitations may be generated by applying Bogoliubov quasiparticle operators in such a way that the constraint on the total fermionic number is obeyed. Similar to modes in the even sector, $k \in K_+$, the subspace of each mode $k \in \bar{K}_+$ yields four eigenstates of H_k and, in principle, a basis formally identical to the one in Eq. (6) for the odd Hilbert-space sector. Although for finite N (thus necessarily in numerical simulations) $\mathcal{P}$ is always a good quantum number under dynamics induced by H, the error in the computation of observables arising from identifying the two sets of modes K and $\bar{K}$ scales like $1/N$. Thus for sufficiently large N, a simplified description in terms of a unique set of momentum modes is possible by using the basis

$$\mathcal{B} \equiv \bigotimes_{k\in K_+}\mathcal{B}_k \quad (8)$$

to characterize arbitrary states in the full Hilbert space $\mathcal{H} = \bigotimes_{k\in K_+}(\mathcal{H}_k \otimes \mathcal{H}_{-k})$. This becomes accurate in the thermodynamic limit $N \to \infty$, where the many-body ground state becomes twofold degenerate and the $\mathbb{Z}_2$ symmetry spontaneously breaks, causing different $\mathcal{P}$ sectors to mix.
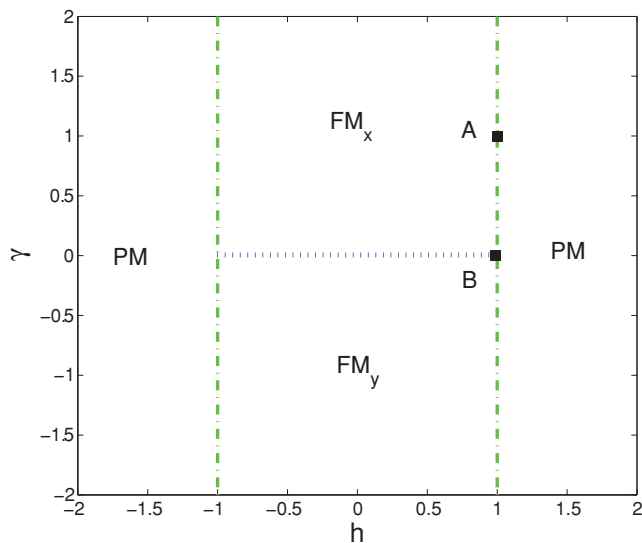
FIG. 2. (Color online) The phase diagram of the XY Hamiltonian in Eq. (2). The regular QCP A ($h_c = 1, \gamma_c = 1$) and the MCP B ($h_c = 1, \gamma_c = 0$) are marked. The dashed-dotted (green) line separates the ferromagnetic (FM) and paramagnetic (PM) phases, whereas the dotted (blue) line represents the superfluid phase (SF).

The equilibrium phase diagram of the model Hamiltonian in Eq. (2) is determined by the behavior of the excitation gap of each mode, $\Delta_k(h, \gamma) \equiv \epsilon_k(h, \gamma)$, with $\epsilon_k(h, \gamma)$ given in Eq. (5), and is depicted in Fig. 2. Throughout this work, we will mainly investigate scaling behavior in quenches involving either the regular QCP A ($h_c = 1, \gamma_c = 1$), which has equilibrium critical exponents $\nu = z = 1$ and belongs to the $d = 2$ Ising universality class, or the MCP B ($h_c = 1, \gamma_c = 0$), which has $\nu = 1/2, z = 2$ and belongs instead to the Lifshitz universality class.[23] In what follows, we shall refer to the *critical mode k_c* as the mode whose gap $\Delta_k(h, \gamma)$ vanishes in the thermodynamic limit. For both the QCPs A and B of interest, we thus have $k_c = 0$ in the large-N limit.

B. Dynamical response indicators

If the system described by Eq. (2) is driven across a QCP by making one (or both) of the control parameter(s) h, γ explicitly time dependent, excitations are induced as a result of the nonequilibrium dynamics. Since the gap vanishes at the QCP in the thermodynamic limit, this happens no matter how slowly the Hamiltonian changes with time. In Refs. 17 and 28, the excess expectation value relative to the instantaneous ground state was shown to successfully characterize dynamical scaling behavior for a large class of physical observables in adiabatic quenches originating from the ground state. That is, for an extensive observable $\mathcal{O}$, the following quantity quantifies the underlying adiabaticity loss:

$$\Delta\mathcal{O}(t) \equiv \langle\Psi(t)|\,\mathcal{O}\,|\Psi(t)\rangle - \langle\tilde{\Psi}(t)|\,\mathcal{O}\,|\tilde{\Psi}(t)\rangle, \qquad (9)$$

where $|\Psi(t)\rangle$ and $|\tilde{\Psi}(t)\rangle$ are the actual time-evolved state and the adiabatically evolved state resulting from $|\Psi(t_0)\rangle$, respectively. For a generic quench process, where in principle both the time dependence in $H(t)$ and the initial state $\rho(t_0)$ can be arbitrary, it is desirable to characterize the response of the

system in such a way that no excitation is generated by purely adiabatic dynamics,[15] and zero-energy quenches are included as a special case. This motivates extending the definition of Eq. (9) to

$$\Delta\mathcal{O}(t) \equiv \mathrm{Tr}[\mathcal{O}(t)\rho(t)] - \mathrm{Tr}[\mathcal{O}(t)\tilde{\rho}(t)], \qquad (10)$$

where now $\rho(t)$ and $\tilde{\rho}(t)$ are the actual time-evolved density operator and the density operator resulting from adiabatic evolution of $\rho(t_0)$, respectively, and we also allow, in general, for the observable $\mathcal{O}$ to be explicitly time dependent. Let $H(t)|\Psi_i(t)\rangle = E_i(t)|\Psi_i(t)\rangle$ define snapshot eigenstates and eigenvalues of $H(t)$ along a given control path. Then the adiabatically steered state $\tilde{\rho}(t) = \sum_{i,j} \rho_{i,j}(t_0)|\Psi_i(t)\rangle\langle\Psi_j(t)|$, with $\rho_{i,j}(t_0)$ being the matrix elements of the initial state $\rho(t_0)$ in the eigenstate basis $|\Psi_i(t_0)\rangle\langle\Psi_j(t_0)|$ of the initial Hamiltonian $H(t_0)$.

With respect to the basis given in Eq. (8), a generic uncorrelated state in momentum space may be expressed in the form $\rho(t) = \bigotimes_{k \in K_+} \rho_k(t)$, where $\rho_k(t)$ is the four-dimensional density operator for mode k. Relative to a snapshot eigenbasis

$$\mathcal{B}_k(t) \equiv \{|\psi_k^j(t)\rangle\}, \quad j = 0, \ldots, 3,$$

similar to the one given in Eq. (6), but constructed from time-dependent quasiparticle operators such that $\gamma_k(t)|0_k(t)\rangle = 0$, $\gamma_k^\dagger(t)|0_k(t)\rangle = |1_k(t)\rangle$, $\rho_k(t)$ may be expressed as

$$\rho_k(t) = \sum_{i,j=0,3} \rho_{ij,k}(t)|\psi_k^i(t)\rangle\langle\psi_k^j(t)|.$$

Suppose that the time-evolution operator for mode k is $U_k(t)$, that is, $\rho_k(t) = U_k(t)\rho_k(t_0)U_k^\dagger(t)$. Direct calculation shows that $|0_k(t), 1_{-k}(t)\rangle = c_{-k}^\dagger|\mathtt{vac}\rangle$, and $|1_k(t), 0_{-k}(t)\rangle = c_k^\dagger|\mathtt{vac}\rangle$ for all t, which indicates that the snapshot eigenstates belonging to the $\mathcal{P}_k = -1$ eigenvalues are frozen in time, $|0_k(t), 1_{-k}(t)\rangle = |0_k(t_0), 1_{-k}(t_0)\rangle$, $|1_k(t), 0_{-k}(t)\rangle = |1_k(t_0), 0_{-k}(t_0)\rangle$. As long as $\mathcal{P}_k$ is conserved under $H_k(t)$, the even and odd sectors for each k are decoupled. Thus upon letting

$$U_k^\dagger(t)|1_k(t), 1_{-k}(t)\rangle$$
$$\equiv a_{0,k}(t)|0_k(t_0), 0_{-k}(t_0)\rangle + a_{1,k}(t)|1_k(t_0), 1_{-k}(t_0)\rangle,$$

we can evaluate the time-dependent excitation probability for mode k as follows:

$$\begin{aligned}
P_k(t) &\equiv \mathrm{Tr}[\rho_k(t)\gamma_k^\dagger(t)\gamma_k(t)] \\
&= \mathrm{Tr}[\rho_k(t)(|1_k(t), 1_{-k}(t)\rangle\langle1_k(t), 1_{-k}(t)|] \\
&\quad + \mathrm{Tr}[\rho_k(t)|1_k(t), 0_{-k}(t)\rangle\langle1_k(t), 0_{-k}(t)|] \\
&= [\rho_{00,k}(t_0) - \rho_{11,k}(t_0)]|a_{0,k}(t)|^2 + \rho_{11,k}(t_0) \\
&\quad + 2\mathrm{Re}[\rho_{01,k}(t_0)a_{0,k}^*(t)a_{1,k}(t)] + \rho_{33,k}(t_0), \qquad (11)
\end{aligned}$$

where the relationships $|a_{0,k}(t)|^2 + |a_{1,k}(t)|^2 = 1$ and $\rho_{10,k} = \rho_{01,k}^*$ have been exploited. Notice that from the above definition of $a_{0,k}(t)$, it follows that $|a_{0,k}(t)|^2$ is the time-dependent probability that mode k is excited when it is in its ground state at $t = t_0$. Similarly, we may express the adiabatically evolved density operator $\tilde{\rho}(t) = \bigotimes_{k \in K_+} \tilde{\rho}_k(t)$, with $\tilde{\rho}_k(t) = \sum_{i,j=0,3} \rho_{ij,k}(t_0)|\psi_k^i(t)\rangle\langle\psi_k^j(t)|$. Thus the time-dependent excitation probability of mode k relative to the adiabatic path is

simply

$$\tilde{P}_k(t) = \text{Tr}[\tilde{\rho}_k(t)\gamma_k^\dagger(t)\gamma_k(t)]$$
$$= \rho_{11,k}(t_0) + \rho_{33,k}(t_0) \equiv P_k(t_0). \quad (12)$$

Upon combining Eqs. (11) and (12), the *relative excitation probability* of mode k is given by

$$\Delta P_k(t) \equiv P_k(t) - P_k(t_0)$$
$$= [\rho_{00,k}(t_0) - \rho_{11,k}(t_0)]|a_{0,k}(t)|^2$$
$$+ 2\text{Re}[\rho_{01,k}(t_0)a_{0,k}^*(t)a_{1,k}(t)]. \quad (13)$$

Physically, a nonzero contribution $P_k(t_0)$ may account for initial excitations due to either a coherent preparation into an excited state or to a finite temperature T. Clearly, if mode k is initially in its ground state, $P_k(t_0) = 0$, we consistently recover the definitions in Ref. 28 for zero-energy quenches. Two relevant limiting cases of Eq. (13) will play a special role in what follows. First, if mode k is initially in a generic pure state of the form

$$|\psi_k(t_0)\rangle \equiv \sum_{j=0,3} c_{j,k} |\psi_k^j(t_0)\rangle,$$

then $\rho_{00,k}(t_0) = |c_{0,k}|^2$, $\rho_{01,k}(t_0) = c_{0,k}c_{1,k}^*$, $\rho_{11,k}(t_0) = |c_{1,k}|^2$, hence

$$\Delta P_k(t) = (|c_{0,k}|^2 - |c_{1,k}|^2)|a_{0,k}(t)|^2$$
$$+ 2\text{Re}[c_{0,k}c_{1,k}^*a_{0,k}^*(t)a_{1,k}(t)]. \quad (14)$$

Second, if the initial state $\rho(t_0)$ is a statistical mixture, then $\rho_{10,k}(t_0) = \rho_{01,k}(t_0) = 0$, and we have

$$\Delta P_k(t) = [\rho_{00,k}(t_0) - \rho_{11,k}(t_0)]|a_{0,k}(t)|^2. \quad (15)$$

The time-dependent excess expectation value $\Delta\mathcal{O}(t)$ in Eq. (10) may be expressed directly in terms of the relative excitation probability for observables that obey $[\mathcal{O}(t), H(t)] = 0$ at all times. In this work, we shall primarily focus on the following choices:

(1) $\mathcal{O}(t) = \frac{1}{N}\sum_{k\in K^+}[\gamma_k^\dagger(t)\gamma_k(t) + \gamma_{-k}^\dagger(t)\gamma_{-k}(t)]$, leading to the relative total density of excitations:

$$\Delta n_{\text{ex}}(t) = \frac{2}{N}\sum_{k\in K_+}\text{Tr}\{[\rho_k(t) - \tilde{\rho}_k(t)]\gamma_k^\dagger(t)\gamma_k(t)\}$$
$$= \frac{2}{N}\sum_{k\in K_+}\Delta P_k(t), \quad (16)$$

which coincides with $n_{\text{ex}}(t)$ when the initial state is the ground state.

(2) $\mathcal{O}(t) = H(t)$, leading to the relative excitation energy density:

$$\Delta H(t) = \frac{2}{N}\sum_{k\in K_+}\text{Tr}[(\rho_k(t) - \tilde{\rho}_k(t))H_k(t)]$$
$$= \frac{2}{N}\sum_{k\in K_+}\epsilon_k(h(t), \gamma(t))\Delta P_k(t). \quad (17)$$

While $\Delta n_{\text{ex}}(t)$ is especially attractive from a theory standpoint in view of its simplicity (possibly enabling analytical calculations), a potential advantage of $\Delta H(t)$ is that it may be more directly accessible in experiments.

As a representative example of an observable *not* commuting with the system's Hamiltonian, we shall additionally include results on the scaling behavior of the following:

(3) $\mathcal{O} \equiv XX = \frac{1}{N}\sum_{i=1}^N \sigma_x^i\sigma_x^{i+1}$, corresponding to the nearest-neighbor spin correlator per site along the x direction.[17] In the Ising limit ($\gamma = 1$), the operator $\mathcal{N} \equiv (1 - XX)/2$ is a natural measure for the "density of kinks" created by the quench, which directly relates to the number of quasiparticles excited at $h = 0$.[12,14,40] We have

$$\Delta XX(t) = \frac{2}{N}\sum_{k\in K_+}\Delta(-2\cos k\, c_k^\dagger c_k)$$
$$+ \Delta[i\gamma(t)\sin k\, (c_k^\dagger c_{-k}^\dagger - \text{H.c.})]. \quad (18)$$

In principle, the sums in Eqs. (16)–(18) should include all the modes in K_+, as indicated. However, for the purpose of analytically investigating dynamical scaling behavior, it is useful to note that not all the allowed modes will necessarily change their state along the adiabatic quench path, effectively making no contribution to the relative expectation $\Delta\mathcal{O}(t)$. In what follows, we shall refer to the subset of modes $K_R \subseteq K_+$ whose state changes in an adiabatic quench as the *relevant modes*. Let a power-law adiabatic quench process be parametrized as $\lambda(t) - \lambda_c = |t/\tau|^\alpha \text{sgn}(t)$, $\alpha = 1$ corresponding to the standard linear case also discussed in the Introduction. We may relate the number of relevant modes, $N_R \equiv |K_R|$, to the system size and the quench rate via $N_R(N, \tau) \propto N|k_{\max}(\tau) - k_c|$, where $k_{\max}$ is the largest momentum in the relevant mode set. Since adiabaticity breaks at a time scale $\hat{t} \sim \tau^{\alpha\nu z/(\alpha\nu z+1)}$, and the typical gap, $\hat{\Delta} \sim \hat{t}^{-1}$, an accessible excited state contributes to the excitation if and only if its minimum gap along the path, $\tilde{\Delta}_k$, matches with this typical gap, $\tilde{\Delta}_k \sim \hat{\Delta}$. In general,[23] $\tilde{\Delta}_k$ scales as $\tilde{\Delta}_k \sim (k - k_c)^{z_2}$, where z_2 is a genuinely nonstatic exponent. Accordingly, the scaling of $k_{\max}$ can be determined by $\hat{\Delta} \sim (k_{\max} - k_c)^{z_2}$, leading to

$$k_{\max} - k_c \sim \tau^{-\alpha\nu z/[z_2(\alpha\nu z+1)]}. \quad (19)$$

III. QUENCHES FROM A PURE EXCITED STATE

A. Adiabatic quench dynamics from an excited energy eigenstate

Adiabatic quenches from the ground state of the initial Hamiltonian $H(t_0)$ have been extensively studied and are well understood in this model.[14–17,23] In order to explore the role of initialization, a first natural step is to investigate dynamical scaling behavior when the initial state is an excited eigenstate of $H(t_0)$. Since, as remarked, the time evolution of excited components along $|0_k, 1_{-k}\rangle$ and $|1_k, 0_{-k}\rangle$ is trivial, we shall focus on excited energy eigenstates with support only on the even sector of each mode k, that is, on states of the form given in Eq. (7). Noting that there are only two possibilities for each mode, either $c_{0,k} = 1$ or $c_{0,k} = 0$, Eq. (14) yields

$$\Delta P_k(t) = (|c_{0,k}|^2 - |c_{1,k}|^2)|a_{0,k}(t)|^2 = \pm|a_{0,k}(t)|^2, \quad (20)$$

and, correspondingly,

$$\Delta n_{\text{ex}}(t_f) = \frac{2}{N}\sum_{k\in K_R}[\pm|a_{0,k}(t_f)|^2]. \quad (21)$$

Thus the relative excitation density is the same, up to a sign, in two limiting cases: (i) the many-body ground state, corresponding to $c_{0,k} = 1$ for all k and to an overall positive sign in Eq. (21), and (ii) the state where all allowed pairs of quasiparticles are excited, corresponding to $c_{0,k} = 0$ for all k and to an overall negative sign in Eq. (21). Since KZS is known to hold for a linear quench process with initial condition (i), and a global sign difference would not change the scaling behavior, KZS is expected to persist for the maximally excited initial eigenstate (ii) as well. This is to some extent surprising both in view of the fact that such an initial state has zero overlap with the BCS state $|\Psi_0^{(+)}\rangle$, and because one would not *a priori* expect highly energetic eigenstates to be sensitive to the ground-state QPT.

Interestingly, critical properties of excited eigenstates in the XY chain have recently attracted attention in the context of *static* QPTs.[53] Suppose that each excited eigenstate is associated with an ordered binary strings of length $|K| = N$, where 0 (1) represents a mode in its ground (excited) state, respectively. Then a compact description of the eigenstate may be given in terms of the "discontinuities" of a (suitably regularized as $N \to \infty$) characteristic function of the corresponding occupied mode set, where no discontinuity is present when all modes are 0 or 1, and a discontinuity is counted every time the occupation of a given mode changes along the string. Alba *et al.*[53] have analytically proved, in particular, that the block entanglement entropy S_L of an excited eigenstate of the critical XY chain may still obey conformal scaling as in the ground state provided that the number of discontinuities remains *finite* in the thermodynamic limit, that is, $S_L \sim \log L$, where $L \gg 1$ is the block size. Conversely, S_L exhibits noncritical scaling, $S_L \sim L$, when the number of discontinuities becomes itself an extensive quantity as $N \to \infty$. Thus certain highly excited states (including the fully excited state considered above) can still display critical behavior, the number of discontinuities in the *full* set of momentum modes being the essential factor in determining the *static* scaling behavior. While, intuitively, nonanalyticities in the characteristic mode occupation function need not play a direct role for simple observables such as the excitation density, these results still prompt the following question: To what extent does a distinction between "critical" (leading to KZS) and "noncritical" excited eigenstates exist for *dynamical* QPTs?

A key difference with respect to the static situation is that only the *relevant* modes matter in a dynamical QPT, $k \in K_R \equiv [k_c, k_{\max}]$, with $k_{\max}$ given in Eq. (19). In Fig. 3, we present exact numerical results, obtained by direct numerical integration of the time-dependent Schrödinger equation, for
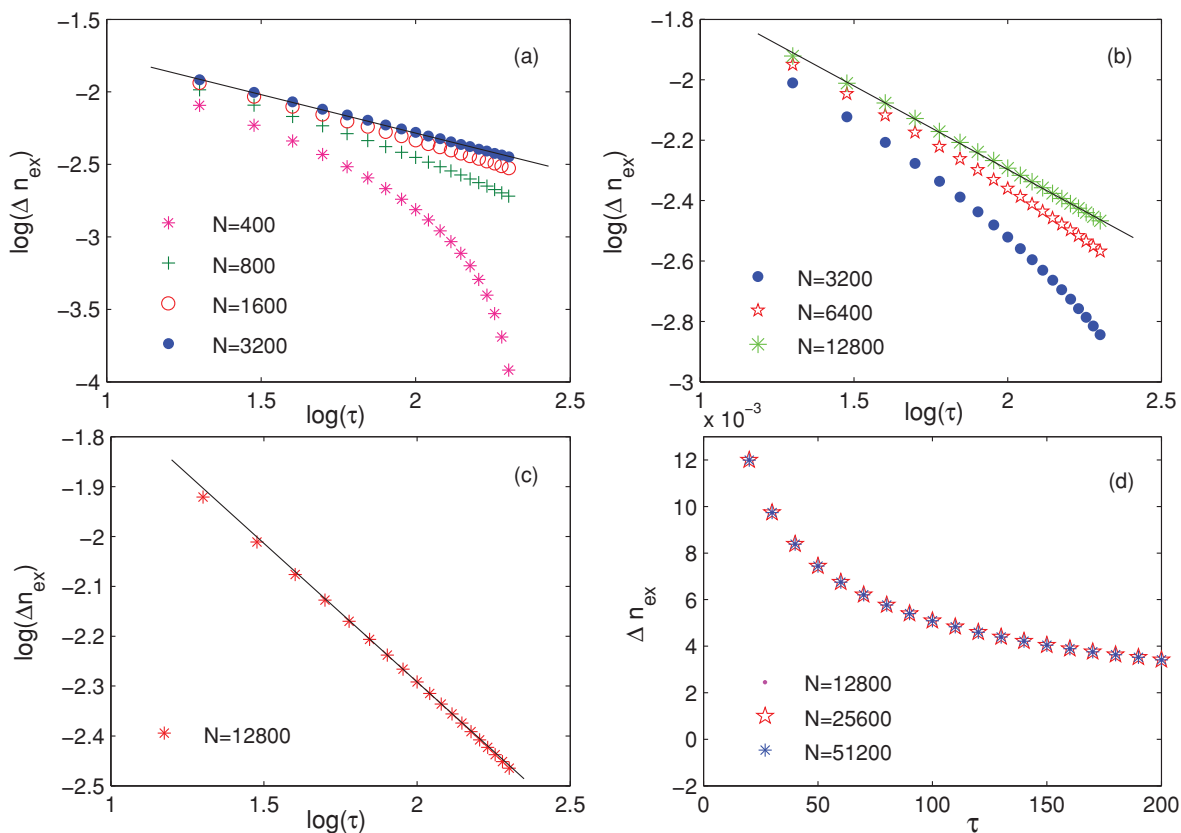

FIG. 3. (Color online) Scaling behavior of the final relative excitation density in a linear quench of the magnetic field h around the QCP A in the Ising chain, starting with different excited eigenstates of $H(h_c)$. (a) Only $k_c = \pi/N$ is excited initially. The linear fit for $N = 3200$ yields -0.535 ± 0.002. (b) The five lowest-energy modes are initially excited. A linear fitting slope of -0.549 ± 0.003 is now reached at $N = 12\,800$. (c) Five modes ($k = k_c$, $5\pi/N$, $9\pi/N$, $13\pi/N$, and $17\pi/N$) are initially excited. The linear fit for $N = 12\,800$ yields -0.546 ± 0.002. (d) The five lowest-energy modes are initially excited for $N = 12\,800$ as in (b), but as the system size is increased linearly, the number of excited modes is increased accordingly. In all cases, the relevant τ range $\tau_{\min} < 20 \leqslant \tau \leqslant 250 < \tau_{\max}$ (see text and Fig. 4).
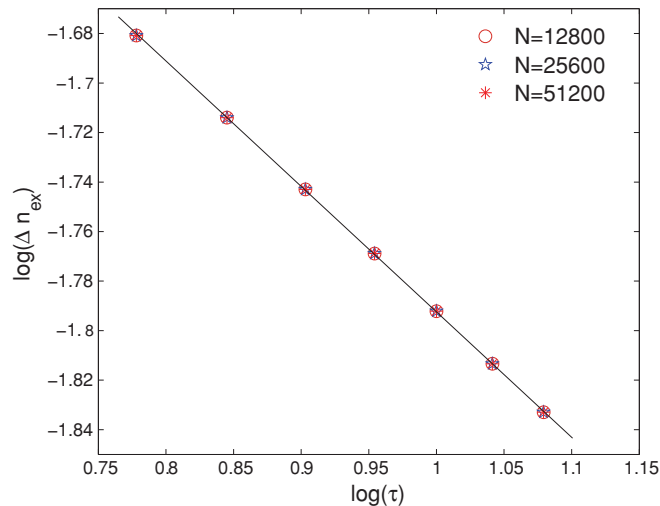
FIG. 4. (Color online) Scaling behavior of the final relative excitation density in a linear magnetic-field quench around the QCP A in the Ising chain, starting with an eigenstate of $H(t_c)$ where the 5, 10, and 20 lowest-energy modes are initially excited for $N = 12\,800, N = 25\,600, N = 51\,200$, respectively [the same as in Fig. 3(d)]. The relevant τ range is now $\tilde{\tau}_{\min} \sim \tau_{\min} = 5 \leqslant \tau \leqslant \tilde{\tau}_{\max} = 20 \ll \tau_{\max}$. A linear fitting slope of -0.5019 ± 0.002 is now reached for all these cases, in agreement with the KZS prediction.

the relative excitation density in a linear adiabatic quench of the magnetic field h around the QCP A of the critical Ising chain ($\gamma = 1$). Different initial eigenstates are compared over a common range of τ, which is chosen to be well within the appropriate τ range[28] for ground-state quenches (see the next paragraph and Fig. 4 for further discussion of this point). In Fig. 3(a), the system is initialized in the first excited state, where only the critical mode is initially excited (thus only one discontinuity is present), whereas in Fig. 3(b), the five lowest-energy modes are initially excited (leading to one discontinuity as well). In case (a), while no scaling is visible for a system with size $N = 400$, progressively better scaling behavior emerges as N is increased, with the value at $N = 3200$ approaching the asymptotic KZS value (and better agreement being achievable by optimizing the τ range, see below). In contrast, for the data in panel (b), a system size as large as $N = 12\,800$ is required for a scaling of comparable quality to be established. Since the only difference between cases (a) and (b) is a different (fixed) number of initially excited modes in N_R, the fact that upon increasing N (thereby increasing N_R accordingly) a better KZS is comparatively obtained in (a) suggests that the *ratio between the number of initially excited (or nonexcited) modes and N_R* is crucial for dynamical scaling behavior—not (as intuitively expected) the discontinuity properties which characterize the initial mode occupation *per se*. More explicitly, let N_E denote the number of modes in K_R that are excited at time t_0, with $N_R - N_E$ correspondingly denoting the number of nonexcited modes in K_R, and let

$$M_R \equiv \min\{N_E, N_R - N_E\}.$$

Motivated by the above observations and also recalling the symmetric role played by initially nonexcited vs excited modes in determining the time-dependent relative probability of excitation [Eq. (20)], we conjecture that KZS emerges

in the thermodynamic limit provided that the initial excited eigenstate satisfies

$$\frac{M_R}{N_R} = \varepsilon \ll 1. \qquad (22)$$

Clearly, the case of ground-state initialization corresponds to $N_E = M_R = 0$, and the fully excited state coincides with $N_E = N_R, M_R = 0$. For a generic initial excited eigenstate, Eq. (22) allows in principle M_R to be an extensive quantity in the thermodynamic limit. Two additional results are included in Fig. 3 to illustrate the above possibility. In panel (c), we still have five excited modes in N_R as in (b), but five discontinuities as opposed to just one. For the same system size (thus also the same ε), the scaling is not worse than in panel (b), further supporting the conclusion that the number of discontinuities does not play a role toward the emergence of dynamical scaling. In panel (d), a fixed value of ε, equal to the one in (b) at $N = 12\,800$, is explored for different values of N, by also proportionally increasing N_E. As the data show, the resulting Δn_{ex} is the same, indicating that M_R may indeed be allowed to be an extensive quantity as long as Eq. (22) is obeyed.

It is important to address how the choice of a range of τ values affects the above scaling conclusions. Let $\tau_{\min} \leqslant \tau \leqslant \tau_{\max}$ and $\tilde{\tau}_{\min} \leqslant \tau \leqslant \tilde{\tau}_{\max}$ denote the valid range for ground-state initialization,[28] and for excited-state initialization, respectively. Since $\tau_{\min}$ is determined from the requirement that an adiabatic regime exists away from criticality, whereas $\tau_{\max}$ follows from ensuring that adiabaticity can be broken in a finite-size system, both $\tau_{\min}$ and $\tau_{\max}$ are related to the scaling of the *many-body* gap between the ground state and first (available) excited state. Thus $\tilde{\tau}_{\min}$ ($\tilde{\tau}_{\max}$) could in general be substantially different from $\tau_{\min}$ ($\tau_{\max}$), respectively. In our case, however, the Hamiltonian in Eq. (2) can be exactly decoupled into two-level systems for each mode k. Therefore the relevant gap is always $\Delta_{k_c} \equiv \varepsilon_{k_c}(h, \gamma)$, *irrespective of the initial condition*. For this reason, the relation $\tau_{\min} \leqslant \tilde{\tau}_{\min}$ and $\tilde{\tau}_{\max} \leqslant \tau_{\max}$ must hold, as any finite-energy initial state might imply more restrictive constraints as compared to the zero-energy case. In particular, according to Eq. (22), not all the excited eigenstates can lead to KZS, and the better Eq. (22) is satisfied, the closer KZS will be approached. This explains why, for instance, the fitting slope -0.549 from Fig. 3(b) is not as close to the KZ value as the one obtained for a ground-state quench with the same range of τ. In the setting of Fig. 3(b), the majority of the relevant modes stay in their ground state. In order to reduce the contribution to Δn_{ex} from the five lowest-energy modes, we can decrease τ such that N_R will be increased in Eq. (22). Numerical support for this strategy is shown in Fig. 4, where an optimal range of τ is identified for the same initial states as in Fig. 3(d), and very good agreement with KZS is recovered. Thus we can conjecture that if the majority of modes that enter M_R are low-energy modes, we can reduce their contribution to Δn_{ex} by decreasing the upper bound to τ. That is, we choose $\tau_{\min} \leqslant \tau \leqslant \tilde{\tau}_{\max}$, where $\tilde{\tau}_{\max} < \tau_{\max}$. Conversely, if the majority of modes that enter M_R are from high-energy modes, then we reduce the contribution from these modes by increasing the lower bound to τ. That is, we let $\tilde{\tau}_{\min} \leqslant \tau \leqslant \tau_{\max}$, with $\tilde{\tau}_{\min} > \tau_{\min}$.

Additional theoretical understanding of the criterion given in Eq. (22) may be sought by invoking the perturbative

adiabatic renormalization (AR) approach,[54] which was successfully applied to explain the scaling results for adiabatic quenches starting from the ground state.[15,28] Can first-order AR still capture dynamical scaling for initial excited eigenstates? Let us focus on linear quenches ($\alpha = 1$), and let the time-dependent Hamiltonian be parametrized as $H(t) = H_c + [\lambda(t) - \lambda_c]H_1 = H_c + (t/\tau)H_1$, with H_c quantum critical in the thermodynamic limit, so that the relevant QCP is crossed at $t_c \equiv 0$. If the system is prepared in the ℓth eigenstate of $H(t_0)$, with $t_0 \to t_c$ as in the examples previously considered, the time-evolved state from first-order AR may be expressed in the form

$$|\Psi^{(1)}(t)\rangle = e^{-i\Gamma_\ell(t)}|\Psi_\ell(t)\rangle - \sum_{m \neq \ell} c_m^{(1)}(t)|\Psi_m(t)\rangle,$$

where $\Gamma_\ell(t)$ includes in general both the Berry phase and the dynamical phase, and $c_m^{(1)}(t)$ gives the time-dependent amplitude along the mth snapshot eigenstate. Following a derivation similar to the one given in Refs. 54 and 28, and letting $\Delta_m(t) \equiv E_m(t) - E_\ell(t)$, we find

$$c_m^{(1)}(t) = \frac{e^{-i\Gamma_m(t)}}{\tau} \int_{t_0}^{t} dt' \frac{\langle \Psi_m(t')|H_1|\Psi_\ell(t')\rangle}{E_m(t') - E_\ell(t')} e^{i \int_{t_0}^{t'} ds \Delta_m(s)}.$$

Thus to first order in the quench rate $1/\tau$ the adiabaticity loss can be quantified by $\Delta \mathcal{O}(t) = \langle \Psi^{(1)}(t)|\mathcal{O}(t)|\Psi^{(1)}(t)\rangle - \langle \Psi_\ell(t)|\mathcal{O}(t)|\Psi_\ell(t)\rangle$. In particular, this yields

$$\Delta n_{\text{ex}}(t) = \frac{2}{N} \sum_{m \neq \ell} \left| c_m^{(1)}(t) \right|^2 \left(\langle \Psi_m(t)| \sum_{k \in K_+} \gamma_k^\dagger(t)\gamma_k(t)|\Psi_m(t)\rangle \right.$$
$$\left. - \langle \Psi_\ell(t)| \sum_{k \in K_+} \gamma_k^\dagger(t)\gamma_k(t)|\Psi_\ell(t)\rangle \right).$$

Since H_1 is a one-body operator in our case, the only nonzero matrix elements $\langle \Psi_m(t)|H_1|\Psi_\ell(t)\rangle$ include many-body eigenstates $|\Psi_m(t)\rangle$ which differ from $|\Psi_\ell(t)\rangle$ in the *occupation of precisely one mode*. Thus $\langle \Psi_m(t)| \sum_k \gamma_k^\dagger(t)\gamma_k(t)|\Psi_m(t)\rangle - \langle \Psi_\ell(t)| \sum_k \gamma_k^\dagger(t)\gamma_k(t)|\Psi_\ell(t)\rangle = \pm 1$, which implies

$$\Delta n_{\text{ex}}(t_f) = \frac{1}{N} \sum_{m \neq \ell} \left[\pm \left| c_m^{(1)}(t_f) \right|^2 \right]. \quad (23)$$

Except for a possible sign difference for each m, the above expression is formally identical to the one holding for ground-state initialization ($\ell = 0$), in analogy with the exact Eq. (21). Numerical calculations of the relative excitation density according to Eq. (23) [for instance, with the same initial condition as in Fig. 3(a), data not shown] confirm that the condition for initial excited eigenstates to support KZS is the same in first-order AR as the one conjectured based on exact numerical results.

B. Sudden quench dynamics from an excited energy eigenstate

As mentioned in the Introduction, scaling results for sudden quenches of the control parameter λ around its critical value λ_c have been recently obtained by De Grandi *et al.*[35] under the assumptions that the system is in the ground state of the initial Hamiltonian and the quench has a *small amplitude*, leading to

a final excitation density

$$n_{\text{ex}}(t_f) \sim |\lambda - \lambda_c|^{d\nu} \equiv \delta\lambda^{d\nu}, \quad (24)$$

with $\delta\lambda \ll 1$ in suitable units. Before addressing, in analogy to the case of adiabatic dynamics, the extent to which the expected scaling behavior may be robust against initialization in a finite-energy eigenstate, it is useful to explore more quantitatively the connection between ground-state adiabatic vs sudden quenches implied by Eq. (24).

Suppose, specifically, that the amplitude of a sudden magnetic-field quench near the QCP A of the Ising chain is directly related to the rate τ of a corresponding linear adiabatic sweep across the same QCP via $h_f = h_c \pm \hat{h}$, where $\hat{h} \propto \hat{t}/\tau$ and $\hat{t}$ is the KZ freeze-out time scale, i.e., $\hat{t} \sim \tau^{\nu z/(\nu z+1)}$. Equation (24) then yields

$$n_{\text{ex}}(t_f) \sim |h_f - h_c|^{d\nu} \sim \tau^{-d\nu/(\nu z+1)}. \quad (25)$$

In other words, the scaling behavior resulting from Eq. (24) is essentially equivalent to KZS. While this could be quantitatively demonstrated by direct calculation of $n_{\text{ex}}(t)$ in a sudden quench, it can also be nicely illustrated by examining *combined* sudden-adiabatic quenches, which have not been explicitly addressed, to our knowledge,[55] and will also be relevant in Sec. III C. Two possible "control loops" starting from $h(t_0) = h_c$ are depicted in Fig. 5: we can either (i) suddenly change the magnetic-field amplitude $h_c \mapsto h_f$, and then adiabatically change it back to h_c (top panel); or we can (ii) slowly ramp up h_c to h_f, and then suddenly quench $h_f \mapsto h_c$ (bottom panel). As is clear from the numerical data, the total excitation density created from the combined sudden-adiabatic quench shows KZS throughout the entire process in both cases, provided that τ is within the appropriate scaling range $\tau_{\text{min}} \leqslant \tau \leqslant \tau_{\text{max}}$. Notice that the quench process depicted in Fig. 5 is similar to the repeated linear quench across QCP A studied in Ref. 19, in the sense that the initial and final value of the control parameter coincide. While KZS was found to hold in such a repeated linear quench, the difference is now that half of the linear adiabatic sweep is replaced by a sudden quench. Since, however, the interval $[h_c - \hat{h}, h_c + \hat{h}]$ corresponds to the impulse region in the KZ scenario for a pure linear quench, the scaling results of the combined quenches under consideration may be understood as a consequence of the fact that the sudden quench component can only further *enforce* the impulse mechanism by which excitation is generated in the KZS argument. Interestingly, as long as the scaling exists, we can also observe that (i) and (ii) lead to almost the same final excitation density, even if the intermediate values of the excitation density after the sole sudden [in (i)] or linear [in (ii)] quench are different. In summary, the existence of KZS in ground-state sudden and combined sudden-adiabatic quenches with *small amplitude* is essentially a reflection of the fact that the system goes through an impulse region around the QCP no matter how slow or fast the quench is effected.

While sudden quenches of *arbitrary amplitude* will be further considered in the next section, we now return to the question of whether dynamical scaling also holds in small-amplitude sudden quenches when the system is initially prepared in an excited eigenstate of $H(t_0) = H_c$. Exact numerical results are presented in Fig. 6, where in order to ease the
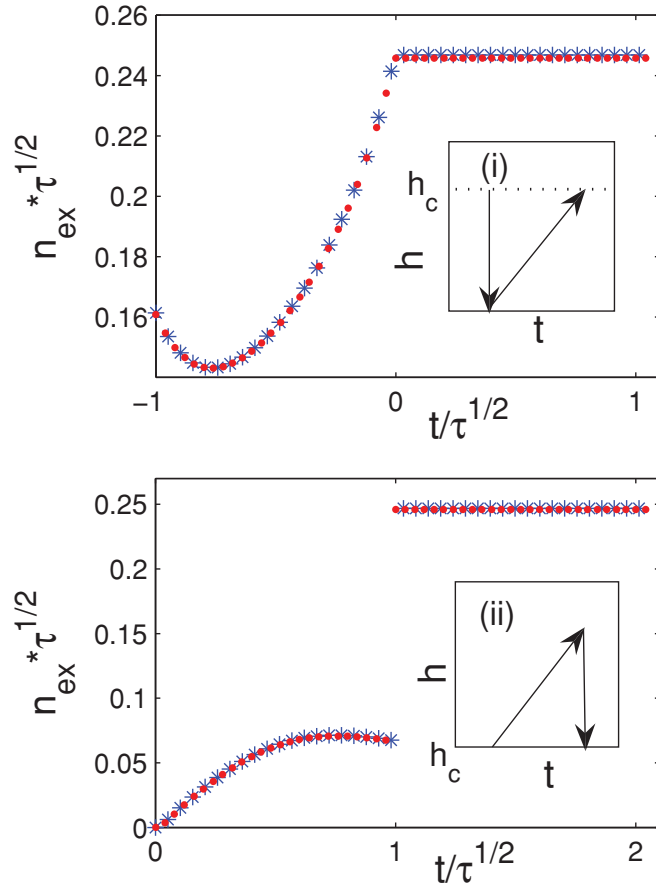
FIG. 5. (Color online): Scaling behavior of the final excitation density in combined magnetic-field ground-state quenches across QCP A in the Ising chain. Top: Sudden quench $h_c \mapsto h_f$ (see text) followed by a linear quench back to h_c, with the system finally kept at h_c. Bottom: Linear quench from h_c followed by a sudden quench $h_f \mapsto h_c$, with the system finally kept at h_c. In both cases, $N = 400$.

comparison with a linear quench, we have again explicitly related the sudden-quench amplitude to τ as $h_f - h_c \propto \tau^{-1/2}$. The data for $N = 3200$ indicate that the scaling exponent is slightly closer to the KZS prediction than the one obtained in a pure linear quench with the same initial condition and τ range [cf. Fig. 3(a)]. Since a sudden quench effectively strengthens the impulse mechanism in the KZS argument, the number of relevant modes N_R is larger than the one involved in an adiabatic linear quench. Thus for the same initial condition (the same M_R), the ratio ε in Eq. (22) is smaller in a sudden quench than in a linear quench, comparatively leading to a scaling exponent closer to KZS. Therefore our conclusions for excited-state sudden quenches are consistent with the ones reached for excited-state adiabatic quenches, and reaffirm how small-amplitude sudden quench dynamics and adiabatic dynamics near a QCP are essentially equivalent over a wide range of initializations.

C. Adiabatic dynamics following a sudden quench from the ground state

In addition to eigenstates of the initial Hamiltonian, another physically relevant class of initial preparations is provided by
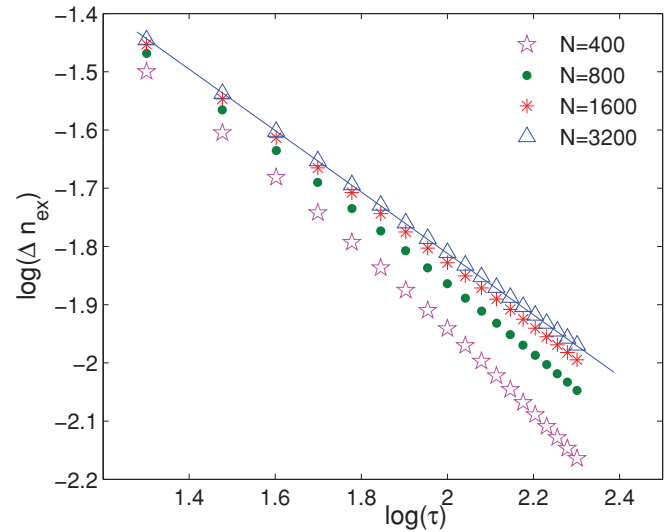

FIG. 6. (Color online) Scaling behavior of the final relative excitation density in a sudden magnetic-field quench across QCP A in the Ising chain, starting with the first excited state of $H(h_c)$. The linear fitting slope for $N = 3200$ is -0.5244 ± 0.0004 for $20 \leqslant \tau \leqslant 250$. Closer agreement with the KZS may be reached by optimizing over τ as in Fig. 4.

pure states that are reachable from the many-body ground state via a sudden parameter quench of *arbitrary amplitude*. For concreteness, let us focus on adiabatic dynamics following a sudden quench of the magnetic field h to its critical value h_c in the Ising chain. Thus the initial state for the adiabatic quench is a superposition of different eigenstates of the Hamiltonian $H(h_c)$ after the (instantaneous) sudden quench. Since for each mode k the parity quantum number $\mathcal{P}_k$ is conserved, and the ground state of H_k lies in the even sector $\mathcal{P}_k = 1$, the expansion coefficients $c_{2,k} = c_{3,k} = 0$, whereas $c_{0,k}$ and $c_{1,k}$ are obtained from expanding the ground state before the sudden quench in the eigenstate basis $\{|\psi_k^j(t_0^+)\rangle\}$ of the quenched Hamiltonian $H(h_c)$.

We can picture the resulting dynamics in terms of a combined sudden-adiabatic quench process (see Fig. 7, inset), except that unlike in Sec. III B we only focus on the scaling behavior of the relative excitation density $\Delta n_{ex}(t)$ created after the sudden quench. Exact numerical results are plotted in the main panel of Fig. 7, showing that for a large range of sudden-quench initializations, the final excitation density still obeys the same KZS,

$$\Delta n_{ex}(t_f) \sim \tau^{-d\nu/(\nu z+1)} \sim \tau^{-1/2},$$

as in adiabatic dynamics starting from the ground state. The above scaling result can be derived analytically in two limiting cases, starting from Eq. (14). Upon integrating over all the relevant modes, we find

$$\Delta n_{ex}(t) = \frac{1}{\pi} \int_0^{k_{max}} \Delta P_k(t) dk = \int_0^{k_{max}} \{(2|c_{0,k}|^2 - 1)|a_{0,k}(t)|^2$$
$$+ 2\text{Re}[c_{0,k} c_{1,k}^* a_{0,k}^* (t) a_{1,k}(t)]\} \frac{dk}{\pi}. \quad (26)$$

There are two contributions in $\Delta P_k(t)$. If the initial state of mode k is close to either a nonexcited or to a fully excited state

($|c_{0,k}|^2 \approx 1$ or $|c_{0,k}|^2 \approx 0$ for all $k \in K_R$, respectively), the first term is the dominant one. In this case, KZS clearly holds. In the opposite limit where each mode $k \in K_R$ is initially half excited ($|c_{0,k}|^2 \approx 1/2$), the second term is the dominant one. Since, for a sudden quench to h_c, the latter is the center of the impulse region (recall Fig. 1, top) and at most half of the impulse region can be crossed, all the relevant modes can at most be close to half excitation, making this second limiting case directly relevant to the sudden-quench state preparation for suitable h_0. Assuming that $|c_{0,k}|^2 \approx 1/2$ and ignoring relative phases thus yields

$$\Delta P_k(t) \sim |a_{0,k}(t) a_{1,k}(t)| \sim |a_{0,k}(t)|\sqrt{1 - |a_{0,k}(t)|^2}.$$

By invoking the Landau-Zener formula,[16] the asymptotic ($t_f \to \infty$) excitation probability for modes near k_c scales like $e^{-2\pi k^2 \tau}$ when $t_0 \to -\infty$. Starting from QCP A (the center of the impulse region) will not, however, affect the exponential behavior.[56] Therefore $|a_{0,k}(t)|^2 \sim e^{-2\pi k^2 \tau}$ as long as t_f is deep in the adiabatic region, and $1 - |a_{0,k}(t)|^2 \sim k^2 \tau$. Integrating over the relevant modes then gives the anticipated KZS result:

$$\int_0^{k_{\max}} dk |a_{0,k}(t)|\sqrt{[1 - |a_{0,k}(t)|^2]} \sim \int_0^{\tau^{-1/2}} dk \, k \, \tau^{1/2} \sim \tau^{-1/2},$$

where we used the fact that $k_{\max} \sim \tau^{-1/2}$ [Eq. (19)] in the upper integration limit.

While the above argument suffices to explain the emergence of KZS starting from *special* sudden-quench initializations, for generic quenches the dominant term in Eq. (26) need not be the same for different modes. In order to gain further insight, it is necessary to inspect the distribution of the excitation probability for each relevant mode after a sudden quench from a generic value $h_0 \mapsto h_c$. Numerical results for the low-lying modes are presented in Fig. 8 for a wide range of initial magnetic-field strength h_0. For each mode k, we can identify two boundary values, $h_{0,k}^{\min}$ and $h_{0,k}^{\max}$, such that when $h_{0,k}^{\min} \leqslant h_0 \leqslant h_{0,k}^{\max}$, mode k is close to its ground state after the sudden quench ($|c_{0,k}|^2 \approx 1$), whereas if $h_0 \ll h_{0,k}^{\min}$ or $h_0 \gg h_{0,k}^{\max}$, mode k is close to half excitation ($|c_{0,k}|^2 \approx 1/2$). Since $h_{0,k}^{\min}$ and $h_{0,k}^{\max}$ are approximately symmetric with respect to the critical value $h_c = 1$, let us for simplicity take $h_{0,k}^{\mathrm{m}} \equiv h_{0,k}^{\max}$, with $h_{0,k}^{\min} \approx 2h_c - h_{0,k}^{\mathrm{m}}$. Qualitatively, $h_{0,k}^{\mathrm{m}}$ can be determined by the condition $\Delta(h_0,k) \approx \Delta(h_c,k)$, which yields approximately $|c_{0,k}|^2 \approx 1$. If, conversely, $\Delta(h_0,k) \gg \Delta(h_c,k)$ ($|h_0 - h_c| \gg |h_{0,k}^{\mathrm{m}} - h_c|$), we can consider $|c_{0,k}|^2 \approx 1/2$. Altogether, the results in Figs. 7 and 8 indicate that the limiting analytical condition of requiring the same dominant term in Eq. (26) for *all* the relevant modes is too strong for $\Delta n_{\mathrm{ex}}(t)$ to show KZS. For instance, when $h_0 = 0.95$, not all the relevant modes are staying in their ground state (k_c is not), yet KZS holds. In general, however, the variation of $|c_{0,k}|^2$ with k does affect the scaling result. For instance, when h_0 is around 0.75, agreement with the KZS prediction for the same system size is relatively poor, motivating one to roughly identify the range $0.6 \lesssim h_0 \lesssim 0.9$ with a crossover region. Based on these observations, we conjecture that a necessary (and sufficient) condition for the relative excitation density $\Delta n_{\mathrm{ex}}(t)$ to approach KZS in the thermodynamic limit is that
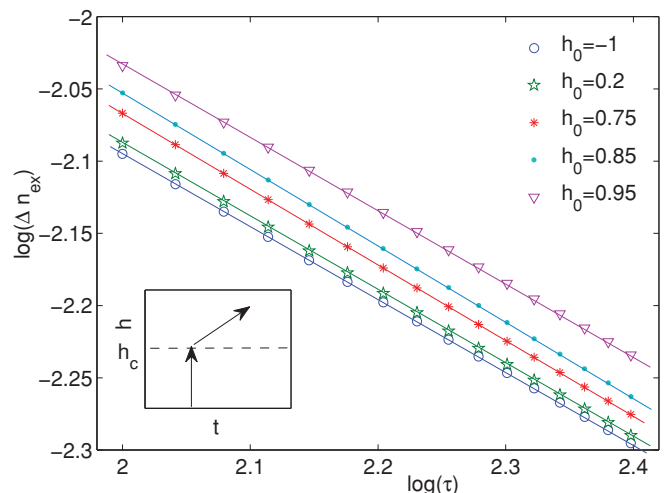

FIG. 7. (Color online) Scaling of the final relative excitation density in an adiabatic magnetic-field quench across QCP A in the Ising chain, starting from an excited state prepared by suddenly quenching $h_0 \mapsto h_c$ for different initial values of h_0. The combined control path is illustrated in the inset. The linear fitting slope for $h_0 = -1, 0.2, 0.75, 0.85, 0.95$ is $-0.50283 \pm 5.0 \times 10^{-5}$, $-0.50697 \pm 6.0 \times 10^{-5}$, $-0.5237 \pm 1.0 \times 10^{-4}$, $-0.52800 \pm 5.0 \times 10^{-5}$, and $-0.5037 \pm 8.0 \times 10^{-4}$, respectively. In all cases, the system size $N = 400$.

the dominant term in Eq. (26) is the same for the majority of the relevant modes.

An alternative physical interpretation of the above conjecture may be obtained by observing that for a generic value of h_0, there exist modes $k_e, k_g \in K_+$ such that if $k_c \leqslant k \leqslant k_e$, $\Delta(h_0,k) \gg \Delta(h_c,k)$, while if $k_g \leqslant k \leqslant \pi$, $\Delta(h_0,k) \approx \Delta(h_c,k)$, and we also assume $k_e < k_g$ for
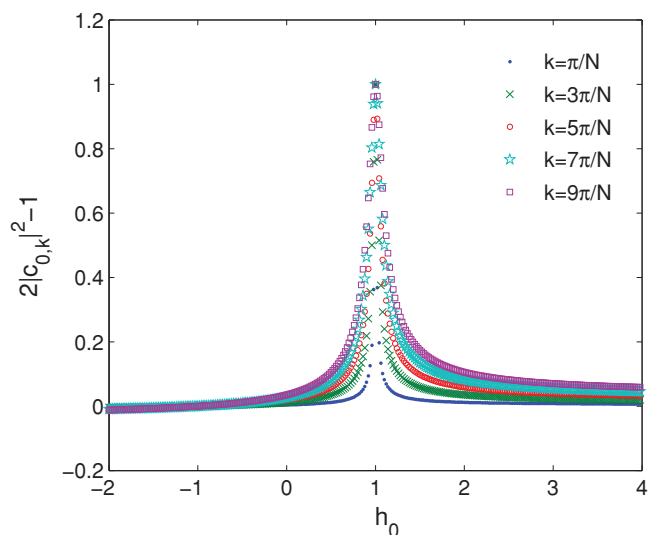

FIG. 8. (Color online) Dependence of the excitation coefficient $2|c_{0,k}|^2 - 1$ upon the initial magnetic-field strength h_0 in a state prepared by a sudden quench $h_0 \mapsto h_c$ in the Ising chain ($\gamma = 1$). The values $c_{0,k}$ are obtained by expanding the ground state of $H(h_0)$ in terms of the eigenbasis of $H(h_c = 1)$ at QCP A. The five lowest-energy modes are considered, for system size $N = 400$.

concreteness. Since, in an adiabatic sweep with speed τ, the set of relevant modes $K_R = [k_c, k_{\max}]$ is determined according to Eq. (19), we can distinguish three different regimes depending on how $k_{\max}$ is positioned relative to the interval $[k_e, k_g]$:

(i) $k_{\max} \leqslant k_e$. In this case, all the relevant modes are half excited, recovering one of the limiting situations (analytically) leading to KZS, as already discussed (e.g., $h_0 = -1$ in Fig. 7);

(ii) $k_e < k_{\max} < k_g$. In this case, by a reasoning similar to the one leading to Eq. (22), KZS is predicted to emerge provided that $(k_{\max} - k_e) = \varepsilon k_{\max}$, $\varepsilon \ll 1$, in such a way that the majority of the relevant modes are half excited (e.g., $h_0 = 0.2$ in Fig. 7);

(iii) $k_g \leqslant k_{\max}$. In this case, KZS is predicted to emerge provided that $k_g = \varepsilon k_{\max}$, $\varepsilon \ll 1$, in such a way that the majority of the relevant modes stay in their ground state (e.g., $h_0 = 0.95$ in Fig. 7).

Thus for both $h_0 = 0.75$ and $h_0 = 0.85$, the initial state prepared by the sudden quench may be interpreted to lie in the crossover region between cases (ii) and (iii), explaining why the resulting scaling deviates appreciably from the KZ prediction.

Similarly to the excited-eigenstate initialization, sudden-quench initialization will also add more constraints on the appropriate τ range for KZS to hold. If the initial state is prepared via a sudden quench that guarantees one of the above conditions (i)–(iii) to be fulfilled for any $\tau \in [\tau_{\min}, \tau_{\max}]$, then the latter range is also appropriate for KZS to emerge under excited-eigenstate initialization. If not, the situation is more involved, and the range of τ may need to be adjusted such that either (ii) or (iii) is enforced. If condition (ii) is more likely to be obeyed (e.g., if $h_0 \approx 0.6$), we can choose $\tilde{\tau}_{\min} > \tau_{\min}$ in such a way that the number of modes between k_e and k_g is decreased, and the majority of relevant modes is thus half excited. If instead condition (iii) is more likely to be obeyed (e.g., if $h_0 \approx 0.9$), we can choose $\tilde{\tau}_{\max} < \tau_{\max}$ in such a way that the number of relevant modes staying in their ground state is increased. While the strategy for adjusting the τ range in a sudden-quench initialization is similar to the one advocated in excited-eigenstate initialization, conditions (i)–(iii) are in fact easier to fulfill than Eq. (22). For instance, for $N = 400$, the worst scaling in Fig. 7 is still relatively close to KZS, whereas the latter is completely lost when initially only k_c is excited in Fig. 3(a). This difference is due to the fact that the initial occupation of modes in the relevant set changes less abruptly in a sudden-quench initialization than in excited-eigenstate initialization.

We conclude our discussion of quench processes originating from a (pure) excited state by commenting on the fact that the analysis developed for $\Delta n_{\mathrm{ex}}(t)$ can be extended to different observables without requiring major conceptual modifications. While an explicit example involving the spin correlator defined in Eq. (18) will be included in the next section, the basic idea is to proceed in analogy with ground-state quenches,[28] by taking into consideration the appropriate scaling exponent as determined by the physical dimension of the observable $\mathcal{O}$. Consider, for instance, the relative excitation energy $\Delta H(t)$ defined in Eq. (17), which, as remarked, can be experimentally more accessible than the relative excitation density. In all the situations where KZS holds for the latter, $\Delta n_{\mathrm{ex}}(t_f) \sim \tau^{-d\nu/(\nu z+1)} \sim \tau^{-1/2}$ (in particular, in the case of excited-state

initialization via a sudden quench just discussed), we also find for our model that

$$\Delta H(t_f) \sim \tau^{-(d+z)\nu/(\nu z+1)} \sim \tau^{-1},$$

consistent with the corresponding ground-state scaling behavior explored in Refs. 28 and 23.

IV. QUENCHES FROM A THERMAL STATE

A. Adiabatic quench dynamics

While we have only focused thus far on initialization mechanisms resulting in a *pure* excited state, another large class of initial states with a finite excitation energy may be obtained through dissipative means, in particular because the system may find itself (or be placed) in contact with a thermal bath. After a time sufficient for equilibration to occur, the system would then relax to a canonical ensemble at temperature T. In equilibrium, it is well known that the influence of a ground-state QCP can cross over to a finite range of temperatures, the so-called "quantum critical regime," which is often broader than naively expected.[1,57,58] In a dynamical scenario, how robust is dynamical scaling (in particular, KZS) to initialization at a finite temperature? If scaling persists, how do the relevant nonequilibrium exponents depend upon the initial temperature? Motivated by these questions, scaling behavior in a system initially prepared in a thermal equilibrium state *at criticality* and then adiabatically quenched away from the QCP has been analyzed in Ref. 35. In particular, it is shown that for fermionic quasiparticles, the excess excitation due to a quench across a standard QCP obeys

$$\Delta n_{\mathrm{ex}}(t_f) \sim \frac{1}{T} \tau^{-(d+z)\nu/(\nu z+1)}, \tag{27}$$

provided that the initial temperature is high enough [$T \gg \epsilon_k(t_0)$, for all $k \in K_R$]. Our goal here is to both present quantitative evidence for the above scaling law and, most importantly, to extend the analysis to multicritical QCPs.

Let T denote the initial thermal equilibrium temperature, so that the initial density operator has the form $\rho(t_0) = \bigotimes_{k \in K_+} \rho_k(t_0)$, with $\rho_k(t_0)$ given by

$$\rho_{00,k}(t_0) = \frac{1}{\mathcal{Z}} e^{+\epsilon_k(h,\gamma)/T}, \quad \rho_{11,k}(t_0) = \frac{1}{\mathcal{Z}} e^{-\epsilon_k(h,\gamma)/T},$$

$$\rho_{22,k}(t_0) = \rho_{33,k}(t_0) = \frac{1}{\mathcal{Z}}, \tag{28}$$

in units where $\hbar = k_B = 1$ and with

$$\mathcal{Z} \equiv 2 + e^{+\epsilon_k(h,\gamma)/T} + e^{-\epsilon_k(h,\gamma)/T}.$$

For clarity, we focus on linear adiabatic dynamics first. We shall study both the standard Ising QCP **A** under a magnetic-field quench of the form $h(t) = 1 - t/\tau$ [$h = h_c = 1, \gamma = 1$ in Eq. (28)], and the MCP **B** under a simultaneous quench of the magnetic field and the anisotropic parameter, $h(t) = 1 - \gamma(t) = 1 - t/\tau$ [$h = h_c = 1, \gamma = \gamma_c = 1$ in Eq. (28)]. At $T = 0$, the scaling of the excitation density can be in both cases described by $n_{\mathrm{ex}}(t_f) \sim \tau^{-d\nu z/[z_2(\nu z+1)]}$], where z_2 is determined from the scaling of the minimal gap along the path with respect to k [cf. Eq. (4) in Ref. 23, with $\alpha = 1$ and $d_2 = 0$]. Thus $z_2 = z$ in the quench across QCP **A**, leading to KZS, whereas $z_2 = 3 \neq z$ in the quench across MCP **B**,

leading to anomalous scaling $n_{\text{ex}}(t_f) \sim \tau^{-1/6}$. Given the above thermal initial condition, starting from Eq. (15) for the relative excitation probability, one finds

$$\Delta P_k(t) = \tanh\left(\frac{\epsilon_k(h_c,\gamma_c)}{2T}\right)|a_{0,k}(t)|^2, \qquad (29)$$

where for both paths we simply write $\epsilon_k(h_c,\gamma_c)$ to mean that critical parameter values are assumed at $t = t_0$. When $T \lesssim \epsilon_k(h_c,\gamma_c)$, $\tanh(\frac{\epsilon_k(h_c,\gamma_c)}{2T}) \approx 1$ and $\Delta P_k(t)$ is the same as starting from the ground state of mode k. Thus in order for the same ground-state scaling (either KZS or $\tau^{-1/6}$) to emerge in the low-temperature limit, the condition $T \lesssim \epsilon_k(h_c,\gamma_c)$ needs to be satisfied for all the relevant modes. Since $\epsilon_{k_c}(h_c,\gamma_c) = 0$, this means that in the thermodynamic limit, the only allowed initial temperature is $T = 0$ if a thermal state of $H(h_c,\gamma_c)$ is considered. In the opposite limit of high temperature, where $T \gg \epsilon_k(h_c,\gamma_c)$, $\tanh(\frac{\epsilon_k(h_c,\gamma_c)}{2T}) \approx \epsilon_k(h_c,\gamma_c)/(2T) \sim (k-k_c)^z/T$ for modes k near k_c. Upon integrating over the relevant modes and recalling Eq. (19), the relative excitation density is then

$$\Delta n_{\text{ex}}(t_f) = \frac{1}{\pi}\int_0^{k_{\max}} \Delta P_k(t_f)d^d k \sim \frac{1}{T}\int_0^{\tau^{-\nu z/[z_2(\nu z+1)]}} k^z d^d k$$

$$= \frac{1}{T}\tau^{-(d+z)\nu z/[z_2(\nu z+1)]}. \qquad (30)$$

For the standard QCP **A**, this yields $\Delta n_{\text{ex}}(t_f) \sim \tau^{-1}/T$, recovering the result of Eq. (27), while $\Delta n_{\text{ex}}(t_f) \sim \tau^{-1/2}/T$ in the multicritical quench across QCP **B**. In Ref. 23, we argued that the time-dependent excitation process in ground-state quenches need not be dominated by the critical mode k_c for certain paths across MCPs and $P_k = \Delta P_k \sim k^{d_2}$, with d_2 playing the role of an "effective dimensionality exponent." For a thermal quench, it is interesting to note that, formally, one may interpret $d_2 = z \neq 0$ in the above equation, also implying that the dominant contribution does *not* originate from modes around k_c. In the high-temperature limit, $\rho_k(t_0)$ is, indeed, almost fully mixed for modes near k_c, causing the contribution of $\rho_{00,k}$ and $\rho_{11,k}$ to Eq. (15) to be nearly canceled, and consistently leading to $\Delta P_k(t) \approx 0$ for those modes.

The scaling prediction in Eq. (30) can be further generalized to a *nonlinear thermal quench*, whereby, for instance, $h(t) = 1 - \gamma(t) = 1 - (t/\tau)^\alpha$ in the case of a quench away from the MCP **B**. When $T = 0$, Eq. (4) in Ref. 23 yields[59] $n_{\text{ex}}(t_f) \sim \tau^{-d\alpha\nu z/[z_2(\alpha\nu z+1)]}$. Correspondingly, in the high-temperature limit,

$$\Delta n_{\text{ex}}(t_f) \sim \frac{1}{T}\tau^{-(d+z)\alpha\nu z/[z_2(\alpha\nu z+1)]}. \qquad (31)$$

Exact numerical results for a quadratic quench ($\alpha = 2$) are reported in Fig. 9, the inset corresponding to the ground-state $T = 0$ case. Within numerical accuracy, the observed behavior is in excellent agreement with the predicted scaling, $\tau^{-2/9}$ for $T = 0$ and $\tau^{-2/3}$ for high-T, respectively.

We further examine how dynamical scaling is detected by other observables and how it is influenced by temperature away from the limiting regimes discussed above by considering the behavior of the spin correlator, $\Delta XX(t)$, defined in Eq. (18). Since XX does not commute with the Hamiltonian in Eq. (2), no analytical treatment is possible. Exact numerical
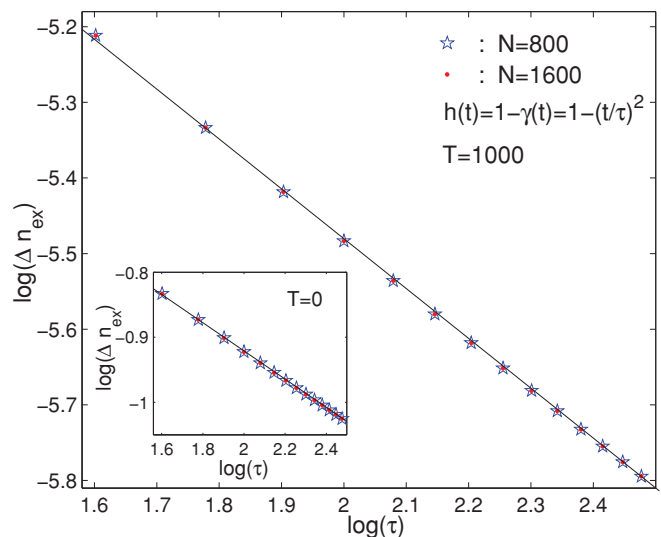

FIG. 9. (Color online) Exact scaling behavior of $\Delta n_{\text{ex}}(t_f)$ in a quadratic adiabatic quench $h(t) = 1 - \gamma(t) = 1 - (t/\tau)^2$, starting from a thermal state at MCP **B** ($t_0 = t_c = 0$) toward the FM phase. The initial temperature $T = 1000$, yielding a linear fitting slope -0.663 ± 0.002, in good agreement with the value $2/3$ predicted by Eq. (31). For comparison, the case of a ground-state quench is reproduced in the inset, with a linear fitting slope of -0.2190 ± 0.0006, which is also in good agreement with the predicted $2/9$ exponent (Ref. 23). The data for different sizes ($N = 800$ and $N = 1600$) coincide up to 10^{-13}.

results are presented in Fig. 10 for both the regular and the multicritical QCPs **A** and **B** (inset vs main panel, respectively), starting from the same thermal initial condition at criticality as considered above. As the data show, similar features emerge in both cases: The scaling exponent of $\Delta XX(t)$, which is expected to be the same as for Δn_{ex}, deviates from its zero-temperature value ($-1/2$ or $-1/6$, respectively) as soon as the temperature is nonzero, and as the latter is gradually increased, it continuously changes until for sufficiently high temperature ($T \gg \epsilon_k(h_c,\gamma_c)$, for all $k \in K_R$), it stabilizes at the value predicted by Eq. (31) (-1 or $-1/2$, respectively). All these observations are consistent with the predictions in the previous paragraph.

In summary, ground-state dynamical scaling (and KZS in particular) is fragile with respect to temperature fluctuations if the initial state is a thermal equilibrium state *at criticality*. In this case, the two situations where scaling exists are the zero-temperature and the high-temperature limit, with Eq. (31) holding in the latter regime. This requires *all* the relevant modes to either stay in their ground state or be highly mixed at the initial time, which is a stronger condition in comparison to the ones identified in the previous sections for coherently prepared (pure) excited states. From a practical standpoint, the high-temperature regime could potentially be relevant to liquid-state NMR simulators.[50] In order for tests of dynamical scaling or KZS in the low-temperature regime to be experimentally viable, however, the initial thermal state needs to be (or be prepared) sufficiently *far away from criticality* (e.g., $|h_0 - h_c| \gg 1$ for QCP **A**), in such a way that the condition $T \lesssim \Delta(k,h_0)$ for all $k \in K_R$ can still be fulfilled with a nonzero temperature.
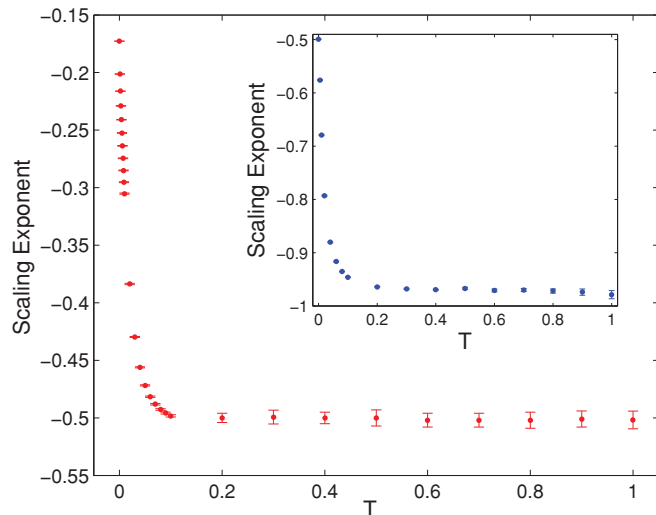
FIG. 10. (Color online) Main panel: Scaling exponent $\Delta XX(t_f)$ as a function of temperature T in a linear quench $h(t) = 1 - \gamma(t) = 1 - t/\tau$ away from the MCP B, starting with a thermal equilibrium state of $H(h_c, \gamma_c)$. Inset: Scaling exponent of $\Delta XX(t_f)$ as a function of temperature in a linear quench $h(t) = 1 + t/\tau$ away from the regular QCP A, starting with a thermal equilibrium state of $H(h_c = 1)$. In both cases, the system size $N = 800$.

B. Sudden quench dynamics and thermalization

Sudden quenches have recently attracted considerable interest as a setting for probing the long-time dynamics of isolated many-body systems and the approach to equilibrium.[36,38–42] Since the quadratic Hamiltonian in Eq. (2) describes a simple (noninteracting) integrable model, it is well known that no thermalization can occur in a proper sense, that is, the behavior of *generic* observables is not governed by a conventional statistical equilibrium ensemble.[37,43] The above investigations have nevertheless shown that information about the asymptotic behavior of an appropriate subset of observables may still be encoded in a finite *effective temperature* T_{eff}, independent on the fine details of the initial state and the dynamics but only determined by the total energy of the process. Let $\rho(t_0) \equiv \rho_0$ and H_f denote, respectively, the density operator describing the initial state of the system, and the final Hamiltonian after the (instantaneous) quench. Following Rossini *et al.*,[38] the effective temperature is defined by the requirement that the average energy of the initial state relative to the quenched Hamiltonian equals the one corresponding to a *fictitious* thermal state at temperature T_{eff} in the canonical ensemble, that is,

$$\text{Tr}[\rho_0 H_f] = \text{Tr}[\rho_{T_{eff}} H_f]. \qquad (32)$$

Under the assumption that $T = 0$ initially [that is, ground-state initialization in Eq. (32)], the emergence of effective thermal behavior has been related to the *locality* properties of different physical observables relative to the quasiparticle language that diagonalizes the model.[39,40] For a generic quench in an Ising chain, only nonlocal observables (such as the two-point correlation functions of the order parameter) have been found to thermalize, with both their asymptotic average value and the finite-time transient being determined by *equilibrium* statistical mechanics at T_{eff}. Remarkably, however, thermal

behavior has also been established for certain *local* observables (the transverse magnetization per site, $1/N \sum_j \sigma_z^j$, and the kink density, $\mathcal{N}$) *in quenches toward criticality*, the long-time value being still univocally determined by T_{eff}.

Physically, it is clear that the concept of an effective temperature has a restricted validity and, for the model under investigation, it does not imply that an actual thermal ensemble emerges as a result of a sudden quench followed by free evolution under the quenched Hamiltonian. With that in mind, we further explore in what follows the emergence of effective thermal behavior in *critical* quenches, by focusing on a different local observable and by extending the analysis in two directions: first, initialization in a thermal state at finite $T > 0$ and, second, sudden quenches to a multicritical QCP.

Let us first consider a sudden quench of the magnetic field $h_0 \mapsto h_f$ in the Ising chain ($\gamma = 1$), starting from an initial state of the form given in Eq. (28), and focus on the long-time behavior of the number of quasiparticle excitations with momentum k. Since the corresponding observable commutes with the time-dependent Hamiltonian, the long-time expectation value $\langle \gamma_k^\dagger \gamma_k \rangle$ coincides with the one right after the quench. In order for the latter to be consistent with the equilibrium value at T_{eff}, the following identity must hold:

$$(\rho_{00,k}(t_0) - \rho_{11,k}(t_0))|a_{0,k}|^2 + \rho_{11,k}(t_0) + \rho_{33,k}(t_0)$$
$$= (1 + e^{+\epsilon_k(h_f, \gamma=1)/T_{eff}})^{-1}, \qquad (33)$$

where $|a_{0,k}|^2$ is the excitation probability of mode k due to the quench and Eq. (11) has been used in the left hand-side. The right-hand side is the fermionic thermal equilibrium prediction $\text{Tr}[\rho_{T_{eff}}^k \gamma_k^\dagger \gamma_k]$. Exact numerical results are presented in Fig. 11. Altogether, these data indicate that similar to the behavior of other local observables in a ground-state quench,[39,40] no effective thermalization is observed outside criticality [Figs. 11(c)–11(f)], as expected. Even for a quench toward QCP A, however, the initial temperature T *must be sufficiently high* in order for our chosen observable to thermalize [Figs. 11(a) vs 11(b)].

In order to gain physical insight into what distinguishes a critical vs noncritical quench in our case, and understand why effective thermal behavior fails to emerge outside criticality even for high initial temperature, it is useful to take a closer look at Fig. 11(d): Clearly, the main difference between the equilibrium and the actual quasiparticle distribution arises from momentum modes close to k_c. On the one hand, since $\Delta(k_c, h_f)$ is the smallest gap at h_f, the maximum quasiparticle excitation is expected to occur at k_c from the equilibrium prediction [right-hand side of Eq. (33)]. On the other hand, the peak of the observed distribution is located at modes close to k_c, but not exactly at k_c. Because the system is far from h_c, note that the difference of $\rho_{00,k}$, $\rho_{11,k}$, and $\rho_{33,k}$ for modes close to k_c is negligible. Thus the main difference is due to $|a_{0,k}|^2$, which, as remarked, is the excitation probability of mode k at $T = 0$ after a sudden quench to h_c. Upon re-interpreting $|a_{0,k}|^2 \leftrightarrow 1 - |c_{0,k}|^2$, it is possible to make contact with the results shown in Fig. 8: clearly, the excitation probability of mode k_c changes dramatically for h_0 close to h_c, which suggests that k_c does not contribute appreciably *unless* $h_f = h_c$. Instead, other modes close to k_c can be excited for values $h_f \approx h_c$ at which k_c is not yet excited. Since the
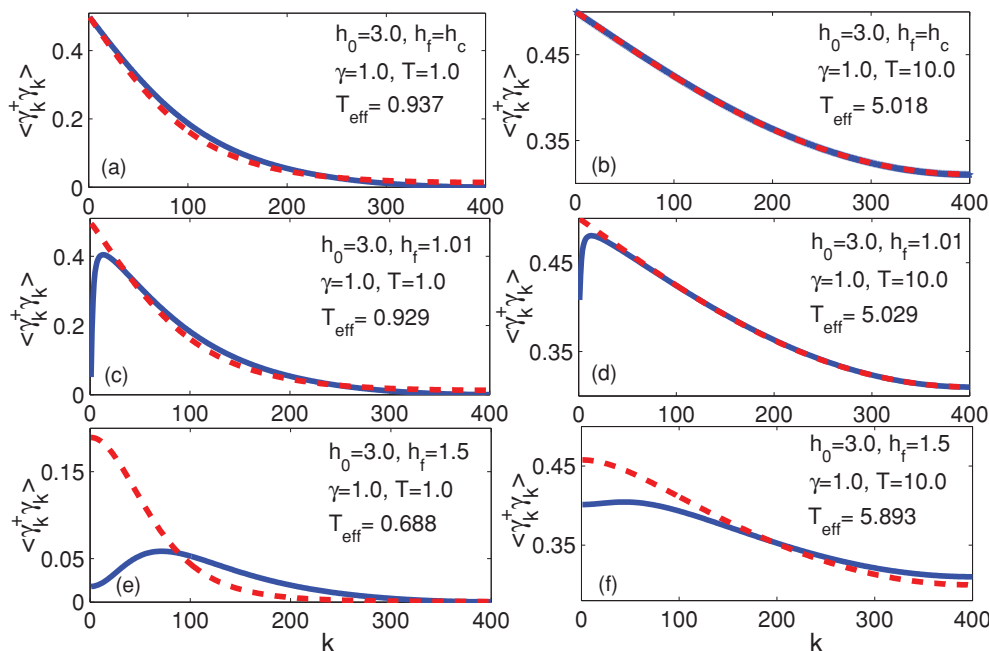
FIG. 11. (Color online) Comparison between the long-time average quasiparticle excitation following a sudden quench $h_0 \mapsto h_f$ starting from a thermal initial state at temperature T (dashed red) and the equilibrium value predicted by a fictitious thermal canonical ensemble at $T_{\rm eff}$ (solid blue). Panels (a), (c), (e): Sudden quenches to $h_f = h_c = 1$, $h_f = 1.01$, $h_f = 1.5$, respectively, with initial temperature $T = 1.0$. The behavior for a ground-state quench ($T = 0$, data not shown) is qualitatively similar, with deviations from the thermal prediction being further pronounced. Panels (b), (d), (f): Sudden quenches to $h_f = h_c = 1$, $h_f = 1.01$, $h_f = 1.5$, respectively, with initial temperature $T = 10.0$. In all cases, $N = 800$, and the value of $T_{\rm eff}$ obtained from is Eq. (32) is also given.

excitation contribution from such "quasicritical modes" would then be larger than the one from k_c, Eq. (33) would not hold. Accordingly, the only way to enforce the validity of Eq. (33) is through a sudden quench toward h_c, as observed.

Having clarified why criticality is essential, we turn to assess whether the requirement of a sufficiently high initial T may be related to the finite system size or will persist in the thermodynamic limit. We focus on a sudden quench $h_0 = 3.0 \mapsto h_c$ at $T = 1.0$, and analyze how the long-time average of the total quasiparticle density $1/N \sum_k \gamma_k^\dagger \gamma_k$ deviates from the thermal equilibrium prediction at $T_{\rm eff}$ as N is increased. While we find that the observed deviations are practically constant over the range of N explored (data not shown), the difference between $\langle \gamma_{k_c}^\dagger \gamma_{k_c} \rangle$ and its corresponding thermal prediction at $T_{\rm eff}$ does decrease with increasing N: As seen in Fig. 12, such a difference $\Delta \gamma_{k_c}^\dagger \gamma_{k_c} \sim N^{-0.99992}$ at $T = 1.0$, implying a vanishing difference and effective thermal behavior also at low temperature *for the critical mode* as $N \to \infty$. This property, however, stems from the fact that the gap of k_c closes in the thermodynamic limit, which is not true for the gap of other modes. For either the number of quasiparticles in a generic mode or for the total quasiparticle density, we thus conjecture that even in the thermodynamic limit, thermal behavior will be observed following sudden quenches to the QCP A *only if* $T \gg \Delta_k(h_c, \gamma = 1)$ *for all the relevant modes*.

In view of the peculiar features that distinguish a multi-critical QCP, as reflected in particular in anomalous scaling behavior,[23] it is not obvious whether the above condition would still suffice for the same observables to thermalize in a sudden quench toward MCP B. Exact results for two

sudden multicritical quenches of the form ($h_0 = 1 + \gamma_0 \mapsto h_f = 1 + \gamma_f, \gamma_0 \mapsto \gamma_f$) are given in Fig. 13, starting from a thermal state at high temperature: Specifically, MCP B is both reached via a sudden quench from the PM phase (left panel) and via a sudden quench from the FM phase (right panel). Contrary to the high-temperature scenario for the
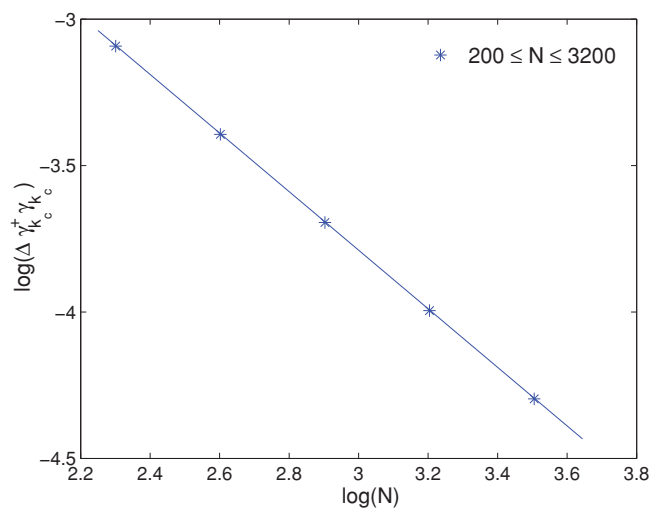

FIG. 12. (Color online) Difference between the long-time quasiparticle excitation of the critical mode k_c from its thermal equilibrium prediction as a function of system size for a sudden magnetic-field quench to h_c in the Ising chain. An initial thermal state with temperature $T = 1.0$ is considered. The linear fitting slope is $-0.99992 \pm 3 \times 10^{-5}$.
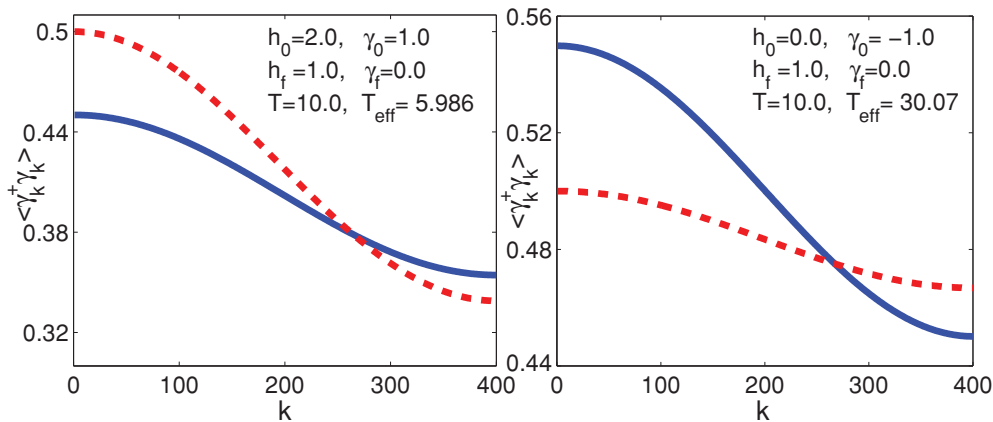
FIG. 13. (Color online) Comparison between the long-time quasiparticle excitation following a sudden quench $h_0 \mapsto h_f = h_c = 1, \gamma_0 \mapsto \gamma_f = \gamma_c = 0$ toward the MCP **B** (blue solid line) and the equilibrium value predicted by a fictitious thermal ensemble at T_{eff} (red dashed line). The system is initially in a thermal state with temperature $T = 10$. Left: Initial state is the thermal state at $h_0 = 2.0, \gamma_0 = 1.0$ (inside the PM phase). Right: Initial state is the thermal state at $h_0 = 0.0, \gamma_0 = -1.0$ (inside the FM phase). Notice that due to the fact that the excitation probability of low-energy modes exceeds $1/2$, T_{eff} is much higher than in any other situation with the same initial T, cf. Figs. 11(b), 11(d), 11(f), and Fig. 13(a).

regular QCP **A** [Fig. 11(b)], *no* thermal behavior emerges, the observed expectation value $\langle \gamma_k^\dagger \gamma_k \rangle$ for modes close to k_c being significantly smaller or larger than the thermal equilibrium prediction, respectively.

This anomalous long-time behavior can be traced back to the asymmetry of the impulse region along the control path, as sketched in Fig. 1 (bottom). Following Ref. 23, the location of the minimum gap for each mode k along the path $h = 1 + \gamma$ is determined by requiring $\partial \Delta_k(\gamma, 1 + \gamma)/\partial \gamma = 0$, that is,

$$\tilde{\gamma}(k) = (\cos k - 1)/(1 + \sin k^2) < 0,$$

which indicates that the center of the impulse region is largely shifted into the FM phase for each k. As a result, after a sudden quench to the MCP **B** from the FM phase, the excitation probability of low-energy modes tends to be enhanced above $1/2$, whereas for a sudden quench to MCP **B** from the PM phase, the excitation probability of low-energy modes tends to be suppressed below $1/2$. Since the thermal equilibrium value is close to $1/2$ in the high-temperature limit for low-energy modes, thermal behavior is not realized in either quench process.

Based on the above results, we conjecture that *quenching toward the center of the impulse region* is a necessary requirement for $\gamma_k^\dagger \gamma_k$ or $1/N \sum_k \gamma_k^\dagger \gamma_k$ to thermalize following a sudden quench. While typically this is the case in a quench to a regular QCP (for instance, a sudden quench of h to QCP **A** at fixed $\gamma = 1$), for a sudden quench to MCP **B** along the path $h = 1 + \gamma$, the location of the minimum gap (hence the center of the impulse region) is different for each mode k, preventing thermalization to be possible along this path irrespective of the final values h_f, γ_f. More generally, we expect the above requirement to be *necessary* for local observables other than those examined here. While this goes beyond our current scope, it would be interesting to verify, for instance, whether the transverse magnetization or the density of kinks would still effectively thermalize in a multicritical quench to QCP **B** from the ground state.

We also remark that in a recent work,[41] general conclusions have been reached for the equilibrium distribution after a sudden quench, predicting, in particular, effective thermal behavior for generic observables when the quench is performed around a noncritical point, and poor equilibration otherwise. While at first these results seem to contradict both our present conclusions for critical quenches toward QCP **A** in the appropriate temperature regime as well as earlier results for zero temperature,[39,40] a crucial assumption in Ref. 41 is a small quench amplitude, causing only a small number of excited states to effectively contribute around a QCP. The opposite condition is implied throughout our discussion, the sudden quench amplitude being in fact large enough for the number of excited states involved in a critical quench to outweigh those involved in a noncritical one (cf. Fig. 8). In light of that, we also conjecture that having a sufficiently large number of states involved in the excitation process is a general necessary condition for effective thermalization after a sudden quench.

V. CONCLUSIONS

In summary, we have addressed how different aspects of many-body nonequilibrium dynamics depend upon initialization in a state other than the ground state for a class of one-dimensional exactly solvable XY models. Our main findings may be itemized as follows:

Dynamical scaling: Initial pure excited states. Provided that the nonequilibrium response of the system is characterized in terms of suitable *relative* indicators (such as the relative excitation density), adiabatic quench dynamics can still encode the ground-state equilibrium critical exponents for a large class of initial energy eigenstates as well as for pure excited states prepared by a sudden parameter quench. A crucial role is played by how the initial excitation is distributed over the set of *relevant* quasiparticle modes that effectively evolve in an adiabatic quench. In particular, a unifying criterion that ensures the emergence of KZS in both of the above scenarios

in the thermodynamic limit is obtained by requiring that the *majority of the relevant modes share a common initial excitation pattern*, as expressed by Eq. (22).

Our results recover ground-state scaling when no excitation is initially present, but they also allow for the critical exponents of the ground-state QPT to be encoded in the scaling behavior for highly energetic initial configurations, where most of the relevant modes are fully or half excited. While this makes contact with similar conclusions on critical entanglement scaling in excited energy eigenstates recently obtained for *static* QPTs,[53] it confirms that only the set of relevant modes is important in dynamical scenarios, as opposed to the full static mode set. Besides being supported by exact numerical methods and analytical derivations in limiting regimes, a justification of the proposed criterion has also been obtained for the case of excited-eigenstate initialization by suitably extending the perturbative (first-order) AR approach we previously employed for ground-state continuous QPTs.

Dynamical scaling: Initial mixed states. In general, more restrictive conditions on the distribution of the initial excitation over relevant modes must be obeyed for universal dynamical scaling to emerge in adiabatic quench dynamics that originates from a statistical (incoherent) mixture as compared to a (coherently prepared) pure state. In particular, two distinct scaling regimes have been identified for an initial thermal ensemble at a finite temperature T, depending on whether the latter is very low or very high relative to the relevant quasiparticle energy scale, and leading to KZS $\tau^{-1/2}$ vs τ^{-1} for a standard QCP, respectively. Since in both cases *all* the relevant modes must share a common excitation pattern if the initial thermal state is prepared *at criticality*, this implies that KZS is fragile against thermal fluctuations in this case, the scaling exponent deviating from the KZ prediction as soon as $T \neq 0$. From a practical standpoint, it is, however, important to note that a finite range of temperatures can still support KZS if the system is initially at thermal equilibrium sufficiently far from criticality. General predictions for scaling behavior in adiabatic thermal quenches involving a MCP have also been obtained [cf. Eq. (31)], and verified to be consistent with exact numerical results.

Effective thermalization. Effective thermal behavior may emerge in the relaxation dynamics of the quasiparticle density following a sudden quench from a thermal state under appropriate conditions. Specifically, the long-time expectation value of this observable is determined by a *fictitious* thermal equilibrium ensemble at temperature T_{eff} provided that (i) the system is quenched toward the *center of the impulse region*, and (ii) the initial temperature is *sufficiently high* with respect to all the relevant gaps. For a standard QCP, the first requirement is met by a sudden quench *toward criticality*, which has been found sufficient for local observables such as the transverse magnetization per site and the kink density to thermalize starting from the ground state.[39,40] Our results indicate that, in general, condition (i) alone need *not* suffice for arbitrary local observables. While requirement (ii) may be taken to be in line with what expected for a free (integrable) theory,[36,43] it remains an interesting open question to precisely characterize what subclass of local observables may exhibit effective thermal behavior under the sole condition (i).[60]

Our results additionally show that for certain observables (such as the quasiparticle density), effective thermalization may fail to occur altogether (or possibly require yet more stringent requirements) for sudden quenches to a *multicritical* QCP. Physically, we have traced this behavior back to the existence of quasicritical (path-dependent) energy states and the corresponding shift of the impulse region, which also underlies the emergence of anomalous scaling exponents.[23] In this context, an interesting next step would be to examine the thermalization behavior of other local observables as considered in Refs. [40] and [39].

While the above analysis provides a more complete picture of nonequilibrium dynamics in a paradigmatic class of spin chains than available thus far, it remains a main open question to understand how crucially our results rely on the XY chain being an exactly solvable noninteracting model. From this point of view, it would be worthwhile to explore, for instance, whether dynamical critical scaling may still exist for finite-energy initial states in nonintegrable models, or even in more complex but still integrable systems such as a Bethe-ansatz solvable one-dimensional Heisenberg XXZ chain[53] or an infinitely coordinated Lipkin-Meshkov-Glick model.[30]

[1] S. Sachdev, *Quantum Phase Transitions* (Cambridge University Press, Cambridge, England, 1999).

[2] M. Vojta, Rep. Prog. Phys. **66**, 2069 (2003).

[3] T. Kadowaki and H. Nishimori, Phys. Rev. E **58**, 5355 (1998).

[4] E. Farhi *et al.*, Science **292**, 472 (2001); G. E. Santoro and E. Tosatti, J. Phys. A **39**, R393 (2006).

[5] E. Barouch and M. Dresden, Phys. Rev. Lett. **23**, 114 (1969).

[6] E. Barouch, B. M. McCoy, and M. Dresden, Phys. Rev. A **2**, 1075 (1970).

[7] E. Barouch and B. M. McCoy, Phys. Rev. A **3**, 2137 (1971).

[8] M. Greiner, O. Mandel, T. Esslinger, T. W. Hänsch, and I. Bloch, Nature (London) **415**, 39 (2002); A. Micheli, G. K. Brennen, and P. Zoller, Nat. Phys. **2**, 341 (2006); L. E. Sadler, J. M. Higbie, S. R. Leslie, M. Vengalattore, and D. M. Stamper-Kurn, Nature (London) **443**, 312 (2006); C. N. Weiler *et al.*, *ibid.* **455**, 948 (2008).

[9] T. Kinoshita, T. Wenger, and D. Weiss, Nature (London) **440**, 900 (2006); S. Hofferberth, I. Lesanovsky, B. Fisher, T. Schumm, and J. Schmiedmayer, *ibid.* **449**, 324 (2007).

[10] W. H. Zurek, U. Dorner, and P. Zoller, Phys. Rev. Lett. **95**, 105701 (2005).

[11] A. Polkovnikov, Phys. Rev. B **72**, 161201 (2005).

[12] J. Dziarmaga, Adv. Phys. **59**, 1063 (2010).

[13] T. Kibble, Phys. Today **60**, 47 (2007).

[14]J. Dziarmaga, Phys. Rev. Lett. **95**, 245701 (2005); B. Damski, *ibid.* **95**, 035701 (2005); B. Damski and W. H. Zurek, Phys. Rev. A **73**, 063405 (2006); R. W. Cherng and L. S. Levitov, *ibid.* **73**, 043614 (2006); F. M. Cucchietti, B. Damski, J. Dziarmaga, and W. H. Zurek, *ibid.* **75**, 023603 (2007); A. Fubini, G. Falci, and A. Osterloh, New J. Phys. **9**, 134 (2007).

[15]A. Polkovnikov and V. Gritsev, Nat. Phys. **4**, 477 (2008).

[16]V. Mukherjee, U. Divakaran, A. Dutta, and D. Sen, Phys. Rev. B **76**, 174303 (2007).

[17]S. Deng, L. Viola, and G. Ortiz, *Recent Progress in Many-Body Theories* (World Scientific, Singapore, 2008), Vol. 11, p. 387.

[18]D. Sen and S. Vishveshwara, Europhys. Lett. **91**, 66009 (2010).

[19]V. Mukherjee, A. Dutta, and D. Sen, Phys. Rev. B **77**, 214427 (2008).

[20]S. Mondal, K. Sengupta, and D. Sen, Phys. Rev. B **79**, 045128 (2009).

[21]R. Barankov and A. Polkovnikov, Phys. Rev. Lett. **101**, 076801 (2008).

[22]U. Divakaran, V. Mukherjee, A. Dutta, and D. Sen, J. Stat. Mech. (2009) P02007.

[23]S. Deng, G. Ortiz, and L. Viola, Phys. Rev. B **80**, 241109(R) (2009).

[24]V. Mukherjee and A. Dutta, Europhys. Lett. **92**, 37004 (2010).

[25]V. Mukherjee, A. Polkovnikov, and A. Dutta, Phys. Rev. B **83**, 075118 (2011).

[26]F. Pellegrini, S. Montangero, G. E. Santoro, and R. Fazio, Phys. Rev. B **77**, 140404 (2008).

[27]S. Mondal, D. Sen, and K. Sengupta, Phys. Rev. B **78**, 045101 (2008); D. Sen, K. Sengupta, and S. Mondal, Phys. Rev. Lett. **101**, 016806 (2008).

[28]S. Deng, G. Ortiz, and L. Viola, Europhys. Lett. **84**, 67008 (2008).

[29]D. Chowdhury, U. Divakaran, and A. Dutta, Phys. Rev. E **81**, 012101 (2010).

[30]T. Caneva, R. Fazio, and G. E. Santoro, Phys. Rev. B **78**, 104426 (2008).

[31]J. Dziarmaga, Phys. Rev. B **74**, 064416 (2006); T. Caneva, R. Fazio, and G. E. Santoro, *ibid.* **76**, 144427 (2007).

[32]B. Damski and W. H. Zurek, New J. Phys. **11**, 063014 (2009); G. Schaller, Phys. Rev. A **78**, 032328 (2008); M. Collura, D. Karevski, and L. Turban, J. Stat. Mech. (2009) P08007; J. Dziarmaga and M. M. Kus, New J. Phys. **12**, 103002 (2010).

[33]A. Das, K. Sengupta, D. Sen, and B. K. Chakrabarti, Phys. Rev. B **74**, 144423 (2006).

[34]Y. Li, M. X. Huo, and Z. Song, Phys. Rev. B **80**, 054404 (2009); H. Guo, Z. Liu, H. Fan, and S. Chen, e-print arXiv:1001.0909 (to be published).

[35]C. De Grandi, V. Gritsev, and A. Polkovnikov, Phys. Rev. B **81**, 012303 (2010).

[36]S. Sotiriadis, P. Calabrese, and J. Cardy, Europhys. Lett. **87**, 20002 (2009).

[37]D. Patané, A. Silva, F. Sols, and L. Amico, Phys. Rev. Lett. **102**, 245701 (2009); M. Rigol, V. Dunjko, and M. Olshanii, Nature (London) **452**, 854 (2008); M. Rigol, Phys. Rev. Lett. **103**, 100403 (2009); M. Cramer, C. M. Dawson, J. Eisert, and T. J. Osborne, *ibid.* **100**, 030602 (2008); M. Kollar and M. Eckstein, Phys. Rev. A **78**, 013626 (2008).

[38]D. Rossini, A. Silva, G. Mussardo, and G. E. Santoro, Phys. Rev. Lett. **102**, 127204 (2009).

[39]S. Suzuki, D. Rossini, and G. E. Santoro, e-print arXiv:0910.4055 (to be published).

[40]D. Rossini, S. Suzuki, G. Mussardo, G. E. Santoro, and A. Silva, Phys. Rev. B **82**, 144302 (2010).

[41]L. Campos Venuti and P. Zanardi, Phys. Rev. A **81**, 032113 (2010).

[42]E. Canovi, D. Rossini, R. Fazio, G. E. Santoro, and A. Silva, e-print arXiv:1006.1634 (to be published).

[43]M. A. Cazalilla and M. Rigol, New J. Phys. **12**, 055006 (2010).

[44]V. Gritsev and A. Polkovnikov, in *Understanding Quantum Phase Transitions* (Taylor & Francis, Boca Raton, 2010); e-print arXiv:0910.3692 (to be published).

[45]D. Patané, A. Silva, L. Amico, R. Fazio, and G. E. Santoro, Phys. Rev. Lett. **101**, 175701 (2008); D. Patané, L. Amico, A. Silva, R. Fazio, and G. E. Santoro, Phys. Rev. B **80**, 024302 (2009).

[46]G. Ortiz, J. E. Gubernatis, E. Knill, and R. Laflamme, Phys. Rev. A **64**, 22319 (2001); R. Somma, G. Ortiz, J. E. Gubernatis, E. Knill, and R. Laflamme, *ibid.* **65**, 42323 (2002).

[47]D. Poulin and P. Wocjan, Phys. Rev. Lett. **102**, 130503 (2009).

[48]P. Zanardi, H. T. Quan, X. Wang, and C. P. Sun, Phys. Rev. A **75**, 032109 (2009).

[49]C. Negrevergne, R. Somma, G. Ortiz, E. Knill, and R. Laflamme, Phys. Rev. A **71**, 032344 (2005).

[50]X. Peng, J. Zhang, J. Du, and D. Suter, Phys. Rev. Lett. **103**, 140501 (2009); J. Zhang, F. M. Cucchietti, C. M. Chandrashekar, M. Laforest, C. A. Ryan, M. Ditty, A. Hubbard, J. K. Gamble, and R. Laflamme, Phys. Rev. A **79**, 012305 (2009).

[51]E. Lieb, T. Schultz, and D. Mattis, Ann. Phys. (NY) **16**, 407 (1961); P. Pfeuty, *ibid.* **57**, 79 (1970).

[52]R. Somma, G. Ortiz, H. Barnum, E. Knill, and L. Viola, Phys. Rev. A **70**, 042311 (2004).

[53]V. Alba, M. Fagotti, and P. Calabrese, J. Stat. Mech. (2009) P10020.

[54]A. Messiah, *Quantum Mechanics* (North-Holland, Amsterdam, 1962), Chap. XVII.

[55]In a recent work by B. Damski, H. T. Quan, and W. H. Zurek, e-print arXiv:0911.5729 (to be published), the behavior of the *decoherence factor* has been advocated as a dynamical indicator of the QPT in an Ising environment. Formally, the required procedure of first turning on the system-environment coupling at the initial time, followed by adiabatic evolution of the Ising chain across the QCP A, can be interpreted in terms of a combined sudden adiabatic quench scheme on the joint system-plus-environment Hamiltonian. Interestingly, KZS is found to occur in the exponent of the decoherence factor as well.

[56]N. V. Vitanov and B. M. Garraway, Phys. Rev. A **53**, 4288 (1996).

[57]S. Sachdev, Nucl. Phys. B **464**, 576 (1996); S. Sachdev and A. P. Young, Phys. Rev. Lett. **78**, 2220 (1997).

[58]P. Gegenwart, Q. Si, and F. Steglich, Nat. Phys. **4**, 186 (2008).

[59]We note that our prediction differs from the one recently established in Ref. 24, where a linearization procedure around the QCP is invoked in order to use the Landau-Zener formula.

[60]From this point of view, it is interesting to note that both the transverse magnetization per site and the density of kinks are closely related to the final quenched Hamiltonian [cf. in particular Eq. (35) in Ref. 40].